2014

Glial fibrillary acidic protein and gliosis: is GFAP more than a marker?

Heather Renee Minkel
University of Alabama at Birmingham

GLIAL FIBRILLARY ACIDIC PROTEIN AND GLIOSIS: IS GFAP MORE THAN A MARKER?

by

HEATHER RENEE MINKEL

MICHELLE OLSEN, COMMITTEE CHAIR
MARK BEVENSEE
MICHAEL BRENNER
JOHN HABLITZ
ERIK ROBERSON

A DISSERTATION

Submitted to the graduate faculty of The University of Alabama at Birmingham,
in partial fulfillment of the requirements for the degree of
Doctor of Philosophy

BIRMINGHAM, ALABAMA

2014

GLIAL FIBRILLARY ACIDIC PROTEIN AND GLIOSIS:
IS GFAP MORE THAN A MARKER?

HEATHER RENEE MINKEL

GRADUATE BIOMEDICAL SCIENCES PROGRAM, NEUROSCIENCE THEME

ABSTRACT

Alexander Disease (AxD) is a 'gliopathy' caused by toxic, dominant gain-of-function mutations in the gene encoding glial fibrillary acidic protein (GFAP). Two distinct types of AxD exist. Type I AxD affected individuals develop cerebral symptoms by four years of age and generally suffer from macrocephaly, seizures, and physical and mental delays. As detection and diagnosis have improved, a larger portion, now about half of all AxD patients diagnosed, have onset >4 years and brainstem/spinal cord involvement. These type II AxD patients typically experience ataxia, palatal myoclonus, dysphagia and dysphonia. To date no study has examined a mechanistic link between the mutations in GFAP and the more caudal symptoms present in patients with type II AxD. Here we demonstrate that two key astrocytic functions, the ability to regulate both extracellular K^+ and glutamate, are compromised in hindbrain regions and spinal cord in AxD mice. Spinal cord astrocytes in AxD transgenic mice are depolarized relative to wild type littermates, and have about a three-fold reduction in Ba^{2+}-sensitive Kir4.1 mediated currents and six-fold reduction in glutamate uptake currents. The loss of these two functions is due to significant decreases in Kir4.1 (>70%) and GLT-1 (>60%) protein expression. The loss of protein is associated with reduced mRNA expression of *KCNJ10* and *SLC1A2*, the genes that code for Kir4.1 and GLT-1, respectively. Gene transcripts for each gene start to show differences at postnatal day 7 in AxD mice and never reach adult WT levels. Protein and mRNA reductions for both Kir4.1 and GLT-1 are

exacerbated in AxD models that demonstrate earlier accumulation of GFAP and increased Rosenthal fiber formation, supporting the notion of GFAP toxicity. We propose these changes cause chronic dysregulation of K^+ and glutamate, providing a mechanistic link between the GFAP mutations/overexpression and the resulting symptoms in those affected with type II AxD.

Keywords: astrocyte, Kir4.1, GLT-1, potassium buffering, glutamate homeostasis, gliosis

DEDICATION

For my family, who gave me the support and encouragement that's made me who I am.

My parents, Ann and Mike Minkel

My grandparents Bonnie and Jim Ashbaugh and Leila and George Minkel

And my siblings, Joseph, Sarah, and Danielle

ACKNOWLEDGMENTS

I have Michelle Olsen to thank for the completion of my Ph.D. She, more than anyone else, has fostered my development as a scientist. Her passion and enthusiasm are contagious, and her hard work a model for success.

My work has been experimentally supported by a number of individuals and groups at UAB; the most essential being Dr. Michael Brenner. I received immeasurable support from lab members, both past and present. I thank Dr. Sini Nwaobi and Dr. Vishnu Cuddapah for all conversations about science and life along the way. I was also fortunate to have the talents of Tooba Anwer and Kara Arps, two neuroscience undergraduate students, to assist in several essential experiments.

I thank my thesis committee for their guidance and expertise – Dr. Mark Bevensee, Dr. Michael Brenner, Dr. John Hablitz, and Dr. Erik Roberson – which has provided me both direction and support throughout.

TABLE OF CONTENTS

Page

LIST OF FIGURES

Figure *Page*

GLIAL FIBRILLARY ACIDIC PROTEIN AND GLIOSIS:
IS GFAP MORE THAN A MARKER?

INTRODUCTION

Alexander Disease

The contribution of astrocyte dysfunction to disease processes has received much attention in the last decade. Astrocytes associated with pathological tissue, often termed reactive astrocytes, are characterized by profound changes in protein expression leading to alterations in the funadamental properties of these cells. Whether these changes, which often persist indefinitely, are beneficial or maladaptive is up for debate. Regardless, the contribution of astrocyte dysfunction to neurodegenerative disorders such as Parkinson's, Alzheimer's, and Huntington's diseases (Rempe and Nedergaard, 2010), as well as recent work in multiple sclerosis (Srivastava et al., 2012) and Amyotrophic Lateral Sclerosis (ALS) (Kaiser et al., 2006), indicate that changes in astrocyte function contribute to disease pathology. One commonality consistently observed in astrocytes in each of these disease processes is an increase in expression of the astrocyte-specific intermediate filament glial fibrillary acidic protein (GFAP). The cause of increased expression is unclear; however, elucidating the relationship between GFAP and Alexander Disease (AxD), the only known disorder to originate in astrocytes, may lead to a clearer understanding.

Alexander Disease (AxD) is a neurological disorder caused by dominant gain-of-function mutations in the gene encoding glial fibrillary acidic protein (GFAP) (reviewed in Brenner et al., 2009 and Flint and Brenner, 2011). Two distinct types, I & II exist

(Prust et al., 2011). Individuals with type I, or early onset AxD, develop symptoms within the first few years of life and typically present with macrocephaly, seizures, and physical and mental delays, and display profound dysmyelination in the frontal lobes. As detection and diagnosis have improved, about half of AxD patients diagnosed have onset throughout the lifespan and demonstrate hindbrain involvement. Symptoms of these type II AxD patients include ataxia, palatal myoclonus, dysphagia and dysphonia, and myelination defects may be restricted to more caudal brain regions or absent (Prust et al., 2011;Graff-Radford et al., 2014). Although first described as a leukodystrophy, a lack of myelin deficits in type II AxD suggests that early onset disrupts myelin formation, while later onset has little or no effect on established myelination. Accordingly, Alexander disease has more recently been referred to as an astrogliopathy (Flint and Brenner, 2011).

Magnetic resonance imaging (MRI) is a key diagnostic tool for Alexander disease. “Typical” MRI features, associated with type I AxD, include white matter changes with frontal predominance, high T1-weighted and low T2-weighted signal in periventricular rim, basal ganglia and thalami abnormalities, brainstem abnormalities, and contrast enhancement of the previously listed regions, optic chiasm, fornix, or dentate nucleus (van der Knaap, 2001). Presence of four of these five findings is clinically sufficient for type I AxD diagnosis (Figure 1). In contrast, the single consistent diagnostic MRI feature of later-onset cases is brainstem and spinal cord atrophy (Figure 2) (Balbi et al., 2008). For patients with classic type I clinical symptoms and MRI features, diagnosis can be confirmed by *GFAP* gene sequencing. Less consistent presentation of type II AxD can sometimes lead to an initial misdiagnosis such as multiple sclerosis. It has been

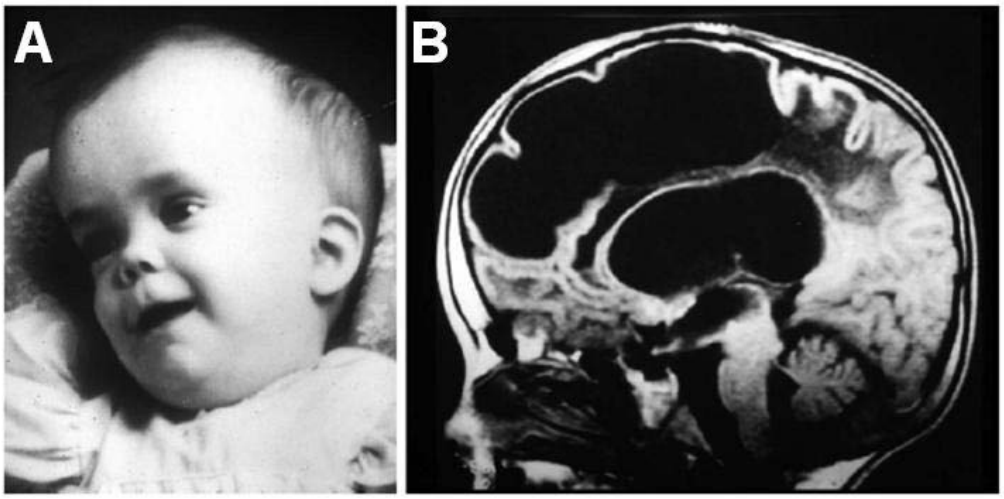

Figure 1. Images of a child with infantile Alexander disease.

This female patient had an R416W mutation (case 10 of Brenner et al., 2001); disease onset was at 3 months, and death was at 8 years. **A.** The patient at 22 months illustrating the frontal bossing and megalencephaly that is often present in infantile cases. **B.** T1-weighted MRI of the patient at 7 years showing cystic degeneration in the frontal lobes, enlarged ventricles, and some atrophy of the vermis.

Note: From Johnson (1996), “Alexander disease,” in: Handbook of Clinical Neurology. pp 701-710, copyright 2004 by Elsevier. Reprinted with permission.

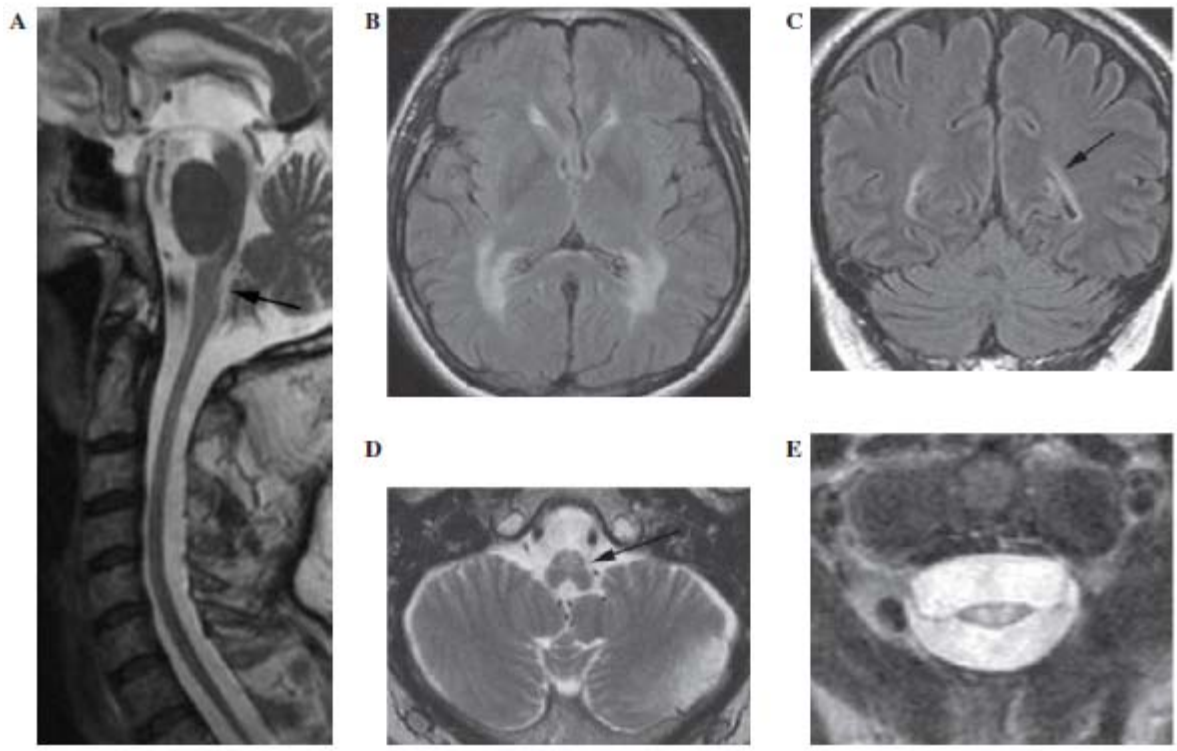

Figure 2. Representative MR images of characteristic lesions of adult onset Alexander disease

A. T2-weighted midline sagittal section shows severe atrophy of the medulla oblongata (*arrow*) and spinal cord. Moderate cerebellar and cerebral atrophy also present. **B.** Axial FLAIR image shows increased signal intensity of the periventricular white matter in posterior regions. **C.** Coronal FLAIR shows thin posterior periventricular white matter, posterior regions. **D.** Axial T2-weighted section demonstrating signal hyperintensities in atrophic anterior medulla oblongata *(arrow)*. **E.** Axial T2-weighted section on cervical spinal cord shows severe atrophy and signal changes at C1-C2 level.

Note: From Pareyson et al. "Adult-onset Alexander disease: a series of eleven unrelated cases with review of the literature." Brain(2008), 131, 2321-2331, copyright 2008 by Oxford University Press. Reprinted with permission.

suggested that the presence of brainstem or spinal cord atrophy by MRI (Pareyson et al., 2008; Balbi et al., 2008) or patients exhibiting progressive ataxia and palatal myoclonus (Balbi et al., 2008;Howard et al., 2008) be considered for type II Alexander disease diagnosis, although ruling out more prevalent disorders remains a common diagnostic route.

Despite large differences in clinical presentation and diagnostic criteria, both types of AxD are unified in the presence of the hallmark pathological feature: GFAP protein aggregates, termed Rosenthal fibers (Wippold et al., 2006). Also found in high abundance within the aggregates are the small heat shock proteins αB-crystallin and HSP27 (Iwaki et al., 1989;Iwaki et al., 1993), and sequestration of phosphorylated c-Jun N-terminal kinase (JNK) and the 20S proteasomal subunit is associated with Rosenthal fibers (Tang et al., 2006). These cytoplasmic inclusions, 10-40μm wide and up to 100μm in length, are believed to originate perinuclear and extend and migrate toward astrocytic endfeet (Figure 3A) (Chin and Goldman, 1996). Pathologically they are generally found in the regions corresponding to observed symptoms: more rostral in type I, and often restricted more to brainstem, cerebellum, and spinal cord in type II (Brenner et al., 2009). Rosenthal fiber formation occurs in areas of highest GFAP expression: the perivascular, periventricular, and subpial regions (Figure 3B) (Wippold et al., 2006;Rizzuto et al., 1980). Before identification of *GFAP* mutations as causal for AxD, autopsy or biopsy confirmation of Rosenthal fibers was necessary for definitive diagnosis.

Mutations in *GFAP* have been identified in about 95% of both type I and type II Alexander disease cases (Brenner et al., 2001;Rodriguez et al., 2001;Gorospe et al., 2002;Li et al., 2005). Reviewed in Brenner et al. 2009, locations of mutations include all

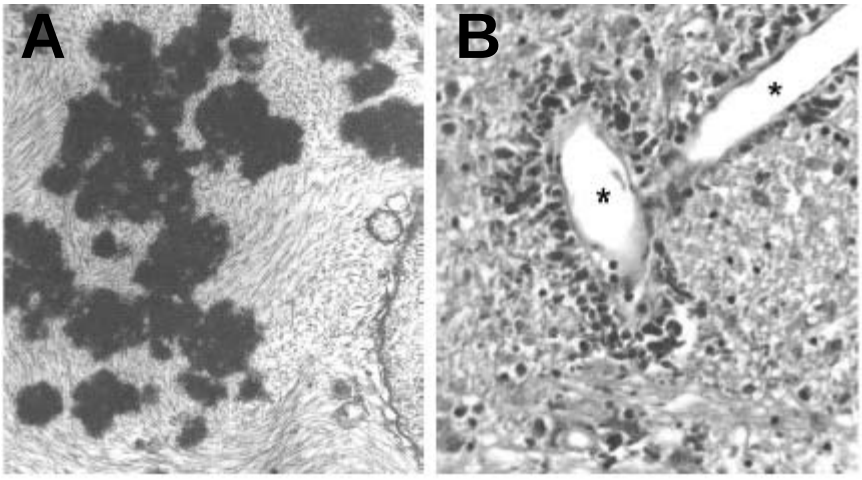

Figure 3. Rosenthal fibers at the light microscopy and electron microscopy level

A. Under EM, Rosenthal fibers appear as membraneless, amorphous osmiophilic aggregates in a dense meshwork of intermediate filaments. **B.** Hematoxylin and eosin staining of the brainstem of a child with R239H mutation reveals Rosenthal fibers as dark nuggets in astrocytic end-feet surrounding blood vessels (asterisks).

Note: From Eng et al (1998), "Astrocytes cultured from transgenic mice carrying the added human glial fibrillary acidic protein gene contain Rosenthal fibers." J Neurosci Res 53:353-360, copyright 1998 by Wiley-Liss. Reprinted with permission.

major functional domains of the protein, most resulting in a single amino acid substitution (Figure 4). The majority of mutations occur *de novo*, and nearly all are 100% penetrant. Two “hot spot” locations, R79 and R239, are most frequently mutated, tend to present with early onset, and for an R239H exchange in particular, rapid progression of disease. On the other hand, a region extending from adjacent coils 1B to 2A contains a number of late-onset inducing mutations. Overall, however, genotype/phenotype correlations are not present for most mutations. Intriguingly, the same mutation may be found in patients that present with either type I or type II AxD.

Mechanisms of disease pathogenesis

The most common disease-causing locations of mutations in *GFAP*, R79 and R236, are homologous to disease-causing mutations in other intermediate filaments (Li et al., 2002). A single mutated allele leads to AxD, as all identified individuals have had heterozygous expression of one mutated and one unaffected allele. This dominant effect of *GFAP* mutations is in contrast to other cytoplasmic intermediate filament disorders, many of which have recessive modes of inheritance, are caused by truncated proteins, and knockout animals exhibit pathology (Li et al., 2002). Here disruption of filament formation suggests a loss of function is responsible for pathology. In contrast, in the brains of AxD patients, normal-appearing GFAP filaments are abundant, even surrounding Rosenthal fibers. In addition, GFAP null mice appear similar to WT littermates, all suggesting a toxic gain of function rather than a loss of normal function driving pathogenesis. Another important observation is the ability of mutations throughout the full length of the protein to result in similar Rosenthal fiber formation in

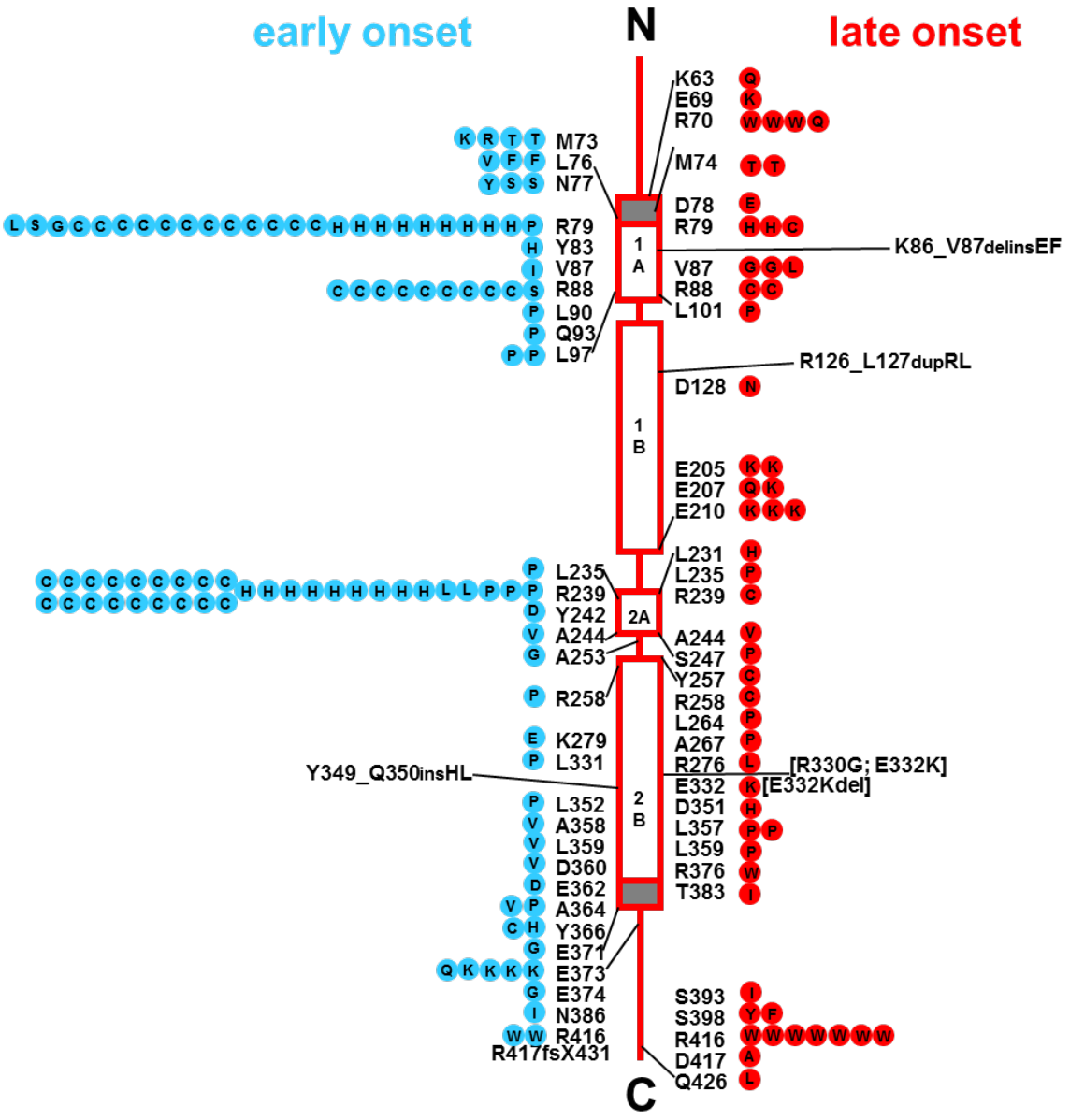

Figure 4. Locations of GFAP mutations in Alexander disease in relation to the protein structure. The 4 open rectangular boxes represent the helical coiled-coil rod domains of GFAP; these structural motifs are highly conserved among most intermediate filament proteins. The solid lines joining these segments are non-helical linker regions, and the solid lines at either end are the nonconserved, random coil, N-terminal and C-

terminal regions. The gray box just before segment 1A is a nonconserved pre-helical sequence important for initiation of rod formation at the start of 1A; the gray box at the end of 2B represents a highly conserved sequence that includes the end of the coiled coil 2B segment. The wild type amino acid is indicated next to the structure, and amino acid replacements within symbols on either side. Early onset cases are on the left, shown as blue circles, and late onset cases are on the right, shown as red circles. Each symbol represents a single patient, except that familial cases, including identical twins, are represented by a single symbol coded for the onset type of the proband.

Note: Courtesy of Dr. Michael Brenner.

the midst of normal GFAP filaments, suggesting interruption of a later-stage of polymerization involving the whole protein (Li et al., 2002). Reduced solubility and salt extraction of GFAP from astrocytes suggests stronger self-adherence in mutant protein, a property that dominantly affects wild type protein when co-expressed, resulting in identical reductions in solubility (Der et al., 2006). A critical threshold of GFAP seems to be necessary for aggregate formation and, unlike other intermediate filament disorders; AxD is confounded by the fact that GFAP itself is upregulated in response to stress in astrocytes. While an increase in GFAP expression may contribute to the ability of cells to form normal filaments in the presence of mutated protein, it seems to ultimately underpin pathology. This creates an opportunity for a toxic, feed-forward pathway of pathological progression. It also provides one mechanism by which disease severity may be modulated by other genetic or environmental factors. Although it may be coincidental, a number of patients have presented clinically following CNS insult including brain trauma or infection (Brenner et al., 2009), suggesting exacerbation by the typical GFAP protein increases in response to acute injury.

Mutant GFAP induces gliotic increases in mutated and non-mutated GFAP expression. As GFAP accumulates, subsequent JNK activation and proteasome inhibition contribute to a cyclic aggravation of the disease process, delineated in Tang et al., 2006. Increased GFAP expression induces cellular stress responses resulting in activation of JNK, known to associate with Rosenthal fibers. Phosphorylated JNK (p-JNK) levels increase relative to total JNK in cells transfected with increasing concentrations of wild type GFAP, and are further increased by R239C mutated GFAP. JNK activation stimulates further GFAP increases, causing inhibition of proteasome

activity. Decreased proteasome function results in additional build-up of GFAP protein. Together a cycle is formed whereby all players are contributing to pathology in a synergistic aggravation of GFAP-induced cellular pathology.

Animal Models of AxD

A number of mouse models have been used to try to elucidate molecular mechanisms of Alexander disease. The first of which, human GFAP overexpressing mice, were discovered to produce Rosenthal fibers and led to the identification of *GFAP* mutations in AxD (Messing et al., 1998;Brenner et al., 2001). A number of human mutation homologs have been inserted into the endogenous mouse gene and shown to be sufficient to produce Rosenthal fibers (Hagemann et al., 2006;Tanaka et al., 2007). A thorough analysis of the relative contribution of both mutation and copy number was performed by Tanaka et al. (2007), in which human R239H GFAP cDNA was expressed under the mouse *GFAP* promoter to generate lines with increasing *hGFAP* copy numbers. A single insertion produced a 3% increase in GFAP and never formed Rosenthal fibers. However, just 2-3 inserts resulted in an approximate 20% increase in protein by postnatal day 7, and 30% by postnatal day 14 when Rosenthal fibers first appeared. This is in contrast to the wild type human GFAP overexpressing mice, where GFAP expression was elevated nearly 4-fold at postnatal day 14, although Rosenthal fibers remained quite diffuse (Messing et al., 1998). This would suggest a direct contribution of mutation to pathological development of Rosenthal fiber formation. While increased GFAP is sufficient to induce aggregation, mutation appears to expedite the process temporally and reduces the threshold of GFAP required for such changes. Using these data, we are also

able to utilize a line crossing the human GFAP overexpressing mice with a mutation knock-in line to compound the effects of these lines into a more severe animal model, resulting in premature death at 3-4 weeks of age (Hagemann et al., 2006).

The GFAP protein

Glial fibrillary acidic protein, a type III intermediate filament protein, is the predominant intermediate filament in astrocytes. One of the longest accepted roles of intermediate filaments is mechanical support, providing strength and maintaining the shape of astrocytes. Highly expressed in this CNS cell type, GFAP is often used as a marker of astrocytes, and increased GFAP expression and astrocytic hypertrophy are characteristic changes indicative of reactive gliosis, associated with essentially any CNS pathology including aging, trauma, and disease (Pekny and Pekna, 2004;Middeldorp and Hol, 2011). Despite this knowledge, relatively little is known about GFAP's functions in normal and pathologic conditions.

In vitro analyses have also begun to demonstrate a role for GFAP in a wide variety of processes (Figure 5). Among these are cell motility (Elobeid et al., 2000;Yoshida et al., 2007), cell proliferation (Messing et al., 1998;Pekny et al., 1998a), vesicle trafficking (Potokar et al., 2008;Potokar et al., 2007), autophagy (Bandyopadhyay et al., 2010), synaptic development (Emirandetti et al., 2006), glutamate uptake and recycling (Hughes et al., 2004;Sullivan et al., 2007;Weir and Thomas, 1984), and blood-brain barrier integrity (Liedtke et al., 1996;Pekny et al., 1998b). Mice that lack or overexpress GFAP have also provided insight into some basic supportive functions the protein provides. GFAP knockout mice, despite complete lack of the intermediate

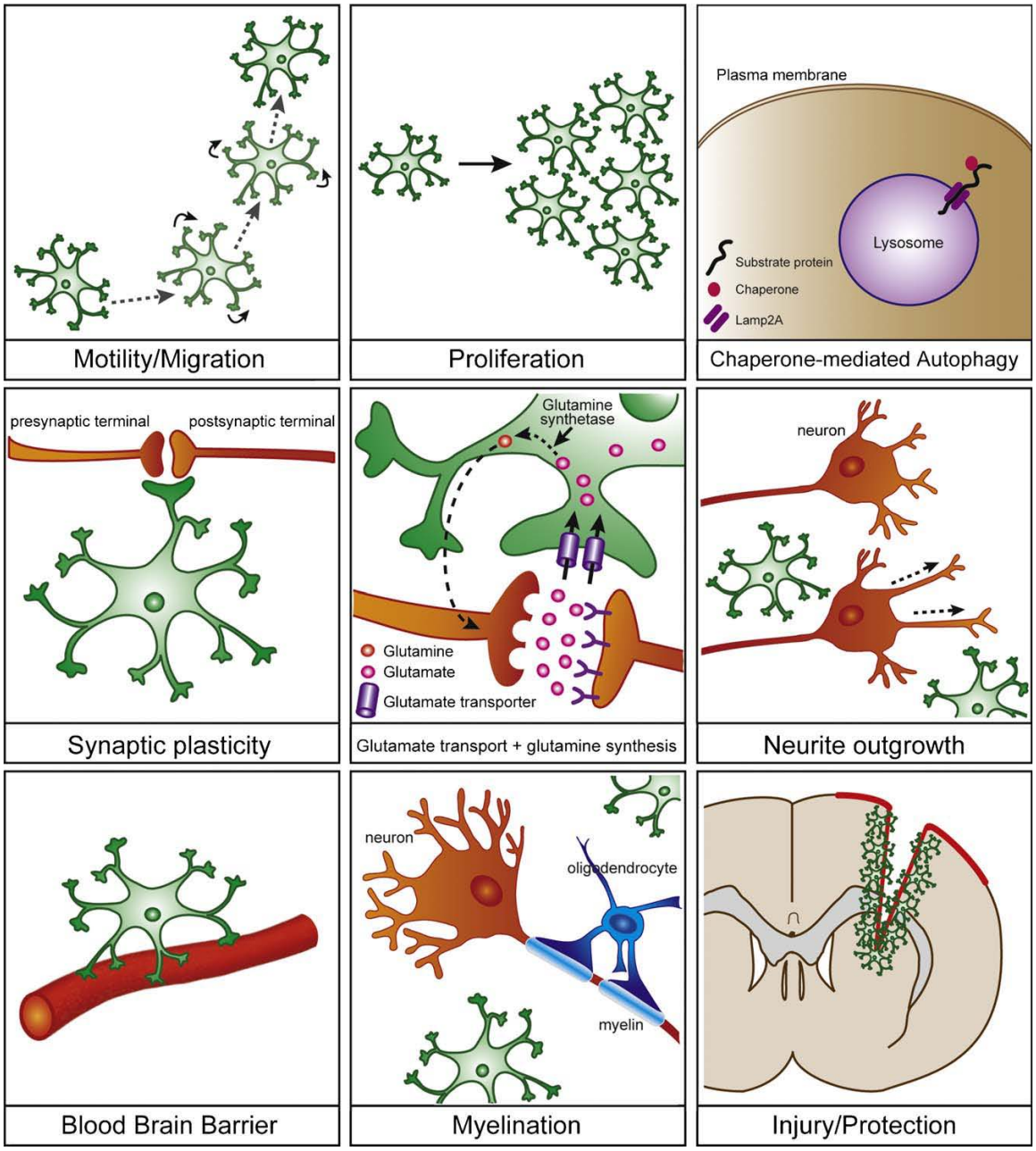

Figure 5. A schematic overview of cellular processes in the brain, in which GFAP has been shown to play a role.

Note: From "GFAP in health and disease" by Middeldorp and Hol, 2011, Prog Neurobiol 93(3):421-43. Copyright 2011 Elsevier. Reprinted with permission.

filament, are largely indistinguishable from wild-type littermates (Liedtke et al., 1996;McCall et al., 1996;Pekny et al., 1998a), however further testing revealed that mice lacking GFAP are more susceptible to cervical spinal cord injury (Nawashiro et al., 2000), cerebral ischemia (Tanaka et al., 2002), and kainic acid-induced excitotoxicity (Otani et al., 2006). Conversely, overexpression of full-length human GFAP causes astrogliotic-like hypertrophy and Rosenthal fiber formation in mice in the absence of precursory trauma or disease (Messing et al., 1998).

In healthy brain, GFAP expression is developmentally upregulated and demonstrates regional differences in promoter activity, mRNA, and protein expression (Palfreyman et al., 1979;Martin and O'Callaghan, 1995;Lein et al., 2007;Jany et al., 2013;Sosunov et al., 2013). Accordingly, brain areas demonstrating most profound pathology and cellular changes in AxD correlate with those regions that developmentally express the highest levels of GFAP (Sosunov et al., 2013;Jany et al., 2013). In humans, caudal brain regions are the most profoundly affected in type II AxD, and in both humans and rodents these regions express the highest levels of GFAP protein and mRNA (Palfreyman et al., 1979;Martin and O'Callaghan, 1995). However, to date, no research has examined astrocytes in caudal brain regions in models of AxD.

Astrocytes

The role of astrocytes in central nervous system function have seen a dramatic change in reputation in the past two decades. Once viewed as structurally, supportive cells, merely filling space between electrically and chemically active neurons, astrocytes are now being identified as increasingly complex and dynamic cells in their own right. It

is clear that while electrically non-excitable, astrocytes still express receptors for nearly all neurotransmitters, and channels that collectively carry a variety of ionic currents. The list of astrocytic roles within the CNS continues to grow and includes many important, neuronally supportive functions. Localization of astrocytic endfeet around neuronal synapses and along blood vessels in combination with gap-junction coupling between astrocytes allows for a polarity that aids in functions including metabolic support, regulation of blood flow, extracellular pH regulation, facilitation of water transport, antioxidant actions, and neurotransmitter uptake, among others, (for full review see (Kimelberg and Nedergaard, 2010)).

Two primary astrocyte functions throughout the CNS, and that are of particular interest in this study, are the ability to buffer or clear K^+ ions and glutamate perisynaptically following periods of neuronal activity. The narrow extracellular space requires each of these functions to be tightly regulated as small increases in extracellular K^+ ($[K^+]_o$) or glutamate ($[Glu^-]_o$) concentrations lead to neuronal dysfunction and modulate the efficacy of neuronal transmission. These processes are largely mediated via the astrocytic inwardly rectifying potassium channel, Kir4.1, and the Na^+-dependent glutamate transporter, GLT-1. Together, these two proteins work in concert to clear the extracellular space of neuronally released K^+ and glutamate and essentially function to dampen neuronal excitability. Dysfunction or inhibition of either protein results in increased neuronal excitability, seizure activity, and at high concentrations for prolonged periods, causes neuronal cell death.

High surface expression of Kir4.1 on astrocytes, paired with the channel's high open-probability and relatively low permeability to Na^+ makes astrocytes particularly

sensitive to changes in $[K^+]_o$. It also contributes to the high resting K^+ conductance and the hyperpolarized resting membrane potential observed in mature astrocytes (Kucheryavykh et al., 2007;Djukic et al., 2007;Kofuji et al., 2000;Olsen et al., 2007). Astrocytes maintain tight regulation of $[K^+]_o$ to around 3mM at rest (Borrelli et al., 1986) and limit accumulation, which occurs proportional to neuronal activity. Two mechanisms have been described for $[K^+]_o$ removal by astrocytes: net uptake, resulting in transient increases in intracellular concentrations; and spatial buffering, through which K^+ is redistributed within the astrocyte syncytium through gap junctions. Kir4.1 is implicated in processes related to maintenance of K^+ homeostasis (Olsen and Sontheimer, 2008). Inhibition or knock down of this channel results in altered extracellular potassium dynamics, depolarized resting membrane potential, and increased input resistance (Djukic et al., 2007; Kucheryavykh et al., 2007; Olsen et al., 2006; Seifert et al., 2009). Kir4.1 knockout animals suffer seizures, ataxia, and early postnatal mortality (Djukic et al., 2007).

The importance of Kir4.1 is further emphasized by a large number of pathologies associated with dysfunction or lack of Kir4.1. Mutations in the protein are associated with SeSAME syndrome (Scholl et al., 2009;Bockenhauer et al., 2009;Reichold et al., 2010), epilepsy (Ferraro et al., 2004;Bordey and Sontheimer, 1998;Hinterkeuser et al., 2000), and autism spectrum disorders (Sicca et al., 2011). Antibodies have been identified in Multiple Sclerosis patients targeted against Kir4.1 (Srivastava et al., 2012b). Potassium dysregulation has been shown to be essential in the pathogenesis of epilepsy (Neusch et al., 2003), ischemia (Sun and Feng, 2013), and Parkinson's disease (Liss et al., 2005), and implicated in Alzheimer's disease (Liu et al., 2010;Etcheberrigaray et al.,

1994) and schizophrenia as well (Tomita et al., 2003). Further, increasing literature indicates loss of Kir4.1 protein consistent with reactive gliosis, associated with a multitude of pathological states (D'Ambrosio et al., 1999;MacFarlane and Sontheimer, 1997;Koller et al., 2000;Pivonkova et al., 2010;Steiner et al., 2012).

The intimate relationship between extracellular glutamate and potassium regulation is emphasized by the observation that the loss or inhibition of Kir4.1 sufficiently depolarizes astrocytes, reducing the electrochemical gradient upon which efficient GLT-1 uptake relies, and thus impairing glutamate uptake (Kucheryavykh et al., 2007;Djukic et al., 2007). This is impressive, as under normal conditions it's difficult to overwhelm glutamate transporters, which even under prolonged high frequency stimulation (Diamond and Jahr, 2000) or repeated 100-fold glutamate challenge *in vitro* (Ye et al., 1999) are able to reduce glutamate concentrations to ambient levels (1-2μM) (Cavelier and Attwell, 2005). These and other data suggest that for glutamate concentrations to rise considerably, GLT-1 must be significantly reduced in expression or function, as it is notably the protein in highest abundance in all of brain (~1.3% of total protein) (Lehre and Danbolt, 1998).

GLT-1 belongs to a family of five excitatory amino-acid transporters (EAATs), of which, one other (GLAST) is also expressed in astrocytes throughout brain. While GLAST is highly expressed in Bergmann glia within the cerebellum, it is more moderately expressed in astrocytes throughout the CNS, and GLT-1 is the predominant astrocytic transporter in adult brain (Anderson and Swanson, 2000). These "sodium dependent" transporters are also influenced by potassium gradients, proton gradients, and membrane potential as both GLT-1 and GLAST move glutamate against its concentration

gradient into astrocytes by coupling transport with movement of these ions down their electrochemical gradients. The result is a net inward positive charge and the astrocytic sodium-potassium pump (Na^+/K^+ ATPase) hydrolyses ATP to maintain Na^+ and K^+ gradients, making the cost of transport more than 1 ATP per glutamate molecule (Sibson et al., 1998).

Once taken up into the astrocyte, two important pathways for glutamate include conversion to glutamine, and entry into the tricarboxylic acid (TCA) cycle (for review see Anderson and Swanson, 2000). The enzyme glutamine synthetase catalyzes conversion of glutamate to glutamine, a process that allows for release from astrocytes and uptake by neurons where it can be turned back into glutamate or further metabolized. Entry of glutamate to the TCA cycle is capable of replenishing the ATP spent for transport into the astrocyte. Also produced by this process are a number of intermediary metabolites including lactate, which can be released from astrocytes and taken up by neurons to be used as an energy substrate (Pellerin and Magistretti, 1994), intricately connecting glutamate uptake to fundamental and essential processes in both astrocytes and neurons.

Perhaps not surprisingly, mice lacking GLT-1 protein exhibit seizures, generalized gliosis, neuronal cell death, hindlimb motor dysfunction, and early postnatal mortality (Tanaka et al., 1997). GLT-1 protein loss may contribute to pathological progression of mouse models of ALS, where it precedes motor neuron cell death. It is also reduced in human ALS patients and corresponds to an increase in CSF glutamate concentrations (Trotti et al., 2001). GLT-1 has also been implicated in the pathology of epilepsy (Ingram et al., 2001), cerebral ischemia (Raghavendra Rao et al., 2000), and Huntington's disease models (Huang et al., 2010). GLT-1 dysfunction is also consistently

coincident with gliosis, including in cases of HIV dementia (Pappas et al., 1998;Wang et al., 2003), hyperammonemia (Hazell et al., 2001), and traumatic injury (McAdoo et al., 2000;Rao et al., 1998). Maragakis and Rothstein, (2004) reviews GLT-1 in many neurologic diseases. The authors note that the ubiquity of glutamate signaling and transporter expression across the CNS may be a partial explanation for transporter dysregulation within such a wide range of seemingly unrelated insults, as it is such a commonly reported finding. However, the role of such dysregulation as a contributing factor or secondary consequence to pathology, (or a combination of both) has been difficult to elucidate

Gliosis

Upregulation of GFAP is the most well characterized and identifiable indicator of gliotic or reactive astrocytes (Pekny and Nilsson, 2005) reliably labeling most, if not all, reactive astrocytes (Sofroniew, 2009). This upregulation of GFAP expression as well as other characteristics of reactive gliosis depends on the particular CNS insult, including severity, immune involvement, whether it is focal or generalized, and acute or chronic (Figure 6) (reviewed in (Burda and Sofroniew, 2014)). Recently Sofroniew (2009) proposed both a definition and model of reactive astrogliosis including the following points: 1) it is a spectrum, and occurs in response to all forms of injury and disease, 2) changes vary by nature and severity of insult along a continuum of gene expression and cellular changes, 3) changes are regulated in a context specific manner, and 4) changes affect both gain and loss of astrocytic functions that can be both beneficial and detrimental to surrounding tissues.

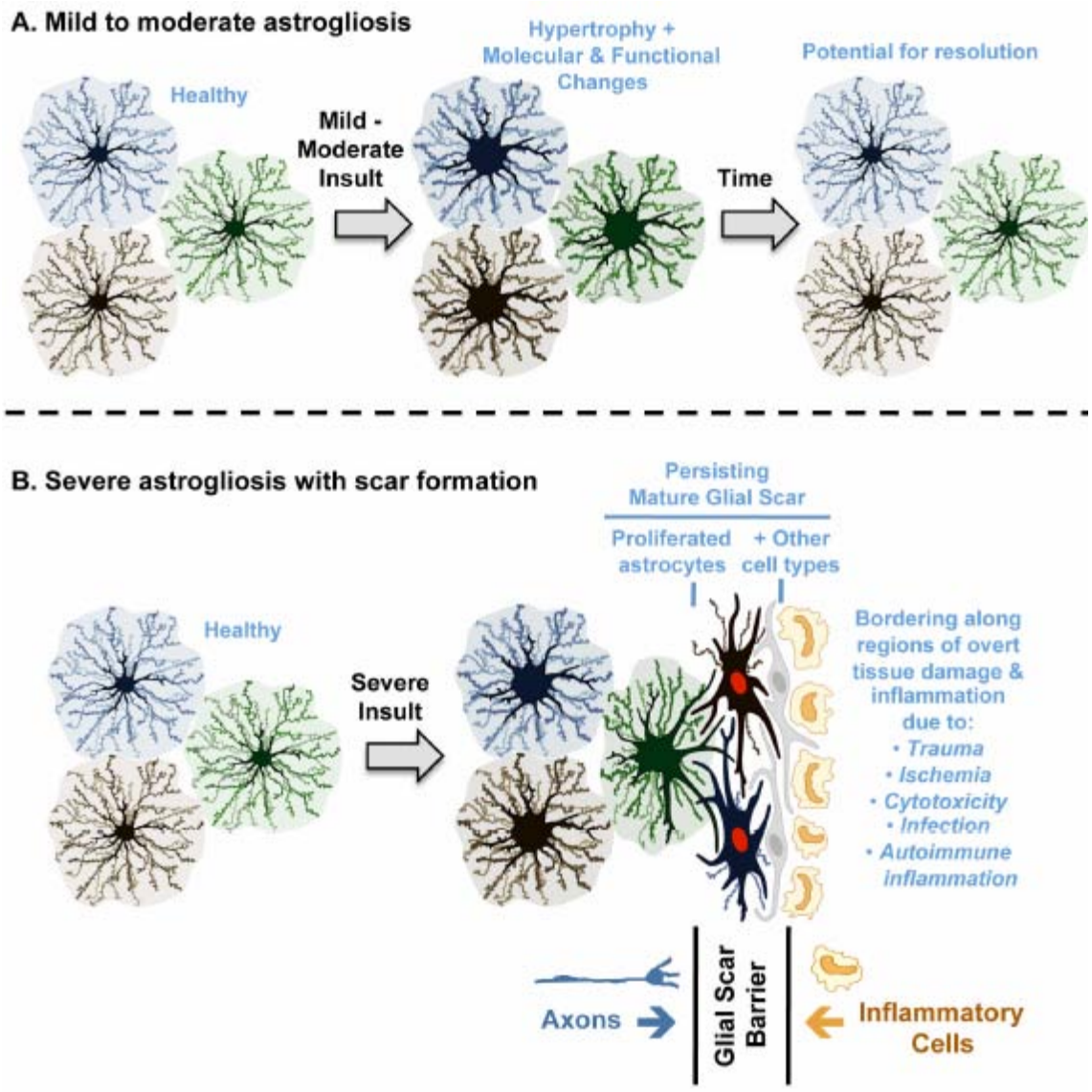

Figure 6. **Schematic representations of different gradations of reactive astrogliosis vary with insult severity.** (A) Mild to moderate reactive gliosis comprises variable changes in molecular expression and functional activity together with variable degrees of cellular hypertrophy. Such changes occur after mild trauma or at sites distant from a more severe injury, or after moderate metabolic or molecular insults or milder infections or inflammatory activation. These changes exhibit the potential for structural resolution if the triggering insult is removed or resolves. (B) Severe reactive astrogliosis with

persisting scar formation generally occurs along borders to areas of overt cell and tissue damage and inflammation. Mature glial scars tend to persist for long periods and act as barriers not only to axon regeneration but also to inflammatory cells in a manner that protects healthy tissue from nearby areas of intense inflammation.

Note: From Sofroniew (2009) “Molecular dissection of reactive astrogliosis and glial scar formation”. Trends in Neurosci. 32(12):638-47. Copyright 2009 by Elsevier. Reprinted with permission.

From releasing inflammatory mediators to cell proliferation, astrogliotic responses are, in fact, quite varied throughout the literature. Many groups have focused recently on the differences in astrocytes in injury and disease models, stressing the heterogeneity of astrocytes and gliosis (Zamanian et al., 2012;Barres, 2008). It is true that even similar changes in astrocytes have contradictory implications in different disease contexts. For example, as reviewed in Sofroniew, 2009, increased GFAP expression can inhibit axonal regeneration in spinal cord injury. Animals lacking astrocytic intermediate filaments GFAP and vimentin show reduced gliosis and increased axonal regeneration following injury (Pekney and Nilsson, 2005; Wilhelmsson et al., 2004). Conversely, these same animals have an exacerbation of experimental autoimmune encephalomyelitis (EAE) severity (Liedtke et al., 1998) and increased lesion size following stroke (Li et al., 2009). All of these data suggest that understanding both changes in astrocytes and their environment must be considered together.

There has also been much focus on common astrocytic responses across families of diseases, such as neurodegeneration, for insight into common pathways and possible mechanistic links that may be conserved (Khakh and Sofroniew, 2014). As listed previously, a wide variety of CNS disorders are associated with reactive astrocytes that demonstrate loss of critical functions of homeostatic glutamate and potassium regulation (Olsen et al., 2010;Dunlop et al., 2003;Tian et al., 2010). In situ, the electrical properties of reactive astrocytes are similar to those seen in immature astrocytes with depolarized resting membrane potentials, reduced K^+ conductance and reduced glutamate uptake (for review see, (Olsen and Sontheimer, 2008)). As a result, recently both Kir4.1 and GLT-1 have become molecular targets for therapeutic intervention. It was recently shown that

selective restoration of Kir4.1 to striatal astrocytes in mouse models of Huntington's disease attenuated some measures of neuronal dysfunction, motor phenotypes, and even lengthened lifespan, identifying astroyctes and Kir4.1 as potential therapeutic targets in Huntington's disease and other neurodegenerative disorders (Tong et al., 2014;Khakh and Sofroniew, 2014). Similarly, GLT-1 protein restoration with Ceftriaxone treatment following traumatic brain injury was associated with decreased gliosis and reduced post-traumatic seizure duration in mice (Goodrich et al., 2013). Moving forward, exploration of AxD, the only identified disorder originating in astrocytes, may provide an interesting perspective to astrocytes and gliosis.

Alexander disease is certainly an example of how gliosis can contribute to pathology. Removed from the context of confounding or precipitating insult or disease, GFAP dysfunction is capable of producing reactive astrocytic phenotypes that ultimately result in disease presentation. It may not be surprising then that AxD shares many features of other disorders. In the case of type II AxD, clinical presentation sometimes leads to misdiagnosis as multiple sclerosis (MS), primary lateral sclerosis, amyotrophic lateral sclerosis (ALS), myasthenia gravis, multisystem atrophy, spinocerebellar ataxia, and cervical myelopathy (Farina et al., 2008; Pareyson et al., 2008). Genetic testing is essential in confirmation of type II AxD, as it is clear that disease presentation and pathological features overlap with a number of other disorders affecting caudal CNS regions. This led to the question: do well-characterized changes in astrocytic potassium and glutamate dynamics occur in AxD as common molecular alterations in caudal CNS pathology?

Hypothesis: AxD results in an extreme form of reactive gliosis, characterized by upregulation of GFAP, and the accumulation of Rosenthal fibers composed of GFAP protein aggregates. Little is known about how this interferes with essential astrocyte functions. Specifically, we will focus on Type II AxD, which until now has been completely unexplored. Here we postulate that gliosis and Rosenthal fiber formation observed in AxD disrupt the ability for astrocytes to maintain extracellular potassium and glutamate homeostasis. We hypothesize that increased GFAP expression/aggregation causes a downregulation in Kir4.1 and GLT-1 expression and function in mouse models of AxD. Chronic dysregulation of K^+ and glutamate may provide a direct mechanistic link between the mutations in GFAP and the resulting symptomology in those affected with AxD. A causal relationship between 'gliosis' and loss of Kir4.1/GLT-1 expression in AxD and may provide valuable information regarding gliosis in the broader context of CNS diseases that present with GFAP overexpression.

METHODS

Animals

All animal procedures and protocols were performed in accordance with the National Institutes of Health guidelines and experiments described here were annually reviewed and approved by the University of Alabama Institutional Animal Care and Use Committee. Mouse lines have been described previously (Messing et al., 1998; Hagemann et al., 2006). Animals were housed with free access to food and water and were maintained on a 12hr light/dark cycle. Genotypes of offspring were confirmed by PCR of DNA isolated from tail (Terra Direct PCR, Clontech).

Slice preparation

Either gender postnatal day (PND) 13-18 pups were anesthetized with CO_2 and decapitated, and the spinal cord was removed and placed in ice-cold, low calcium, artificial cerebral spinal fluid (ACSF, containing in mM, 116 NaCl, 4.5 KCl, 1.0 $MgCl_2$, 0.2 $CaCl_2$, 26.2 $NaHCO_3$, 11.1 glucose, and 5.0 (4-(2-hydroxyethyl)-1-piperazineethanesulfonic acid) (HEPES) sodium salt for 30 s. The cord was then placed in liquid low-melt agar at ~30°C that was quickly solidified by placing on ice. Sections were cut at 300 µm using a Vibratome 3000 (Ted Pella, Redding, CA) in low calcium ACSF. Before recording, slices were allowed to recover for ≥1 hr at room temperature in ACSF containing 2 mM $CaCl_2$, which was continuously bubbled with 5% CO_2-95% O_2.

Slice electrophysiology

Whole cell voltage-clamp recordings were made as described previously (Olsen et al., 2006). Patch pipettes were made from thin-walled (outer diameter 1.5 mm, inner diameter 1.12 mm) borosilicate glass (TW150F-4 World Precision Instruments) and had resistances of 6 – 9 MΩ. Slices were transferred after the recovery period to a Zeiss Axio Examiner D1 microscope with a ×40 water immersion lens to visualize astrocytes. Signals were acquired using an Axopatch 200B amplifier (Axon Instruments) controlled by Clampex 10.2 software via a Digidata 1440A interface (Molecular Devices). Signals were filtered at 2 kHz and digitized at 5 kHz. Data acquisition was conducted with the use of pClamp 10.2 (Axon Instruments). Resting membrane potentials were measured directly from the amplifier in I = 0 mode ~1 min after whole cell access was obtained. Where described in the text, whole cell capacitance and series resistances were also measured directly from the amplifier, with the upper limit for series resistance being 10 MΩ and series resistance compensation adjusted to 80% to reduce voltage errors. Slices were continuously superfused with ACSF with the addition of 2.0 mM $CaCl_2$. The pipette solution contained (in mM) 125 K-Gluconate, 10 KCl, 10 HEPES sodium salt, 10 creatine phosphate, 2 Mg-ATP, 0.2 Na-GTP, and 0.5 EGTA, pH adjusted to 7.3 with KOH and adjusted to 285 -290 mOsm with sucrose. Cells were continuously superfused at 34°C with oxygenated ACSF containing 2 mM $CaCl_2$. Drugs were added directly to these solutions.

Potassium/Glutamate Puffing

Potassium and glutamate solutions were applied for 400 ms using a Picospritzer (Warner Instruments) to astrocytes voltage clamped at -80 mV. The K^+ puffing pipette solution contained 105 mM NaCl, 30 mM KCl, 2 mM $MgCl_2$, 2 mM $CaCl_2$, and 32.5 mM HEPES, pH adjusted to 7.4 with NaOH. The glutamate puffing solution contained 120 mM NaCl, 3.5 mM KCl, 1.3 mM $MgCl_2$, 2.5 mM $CaCl_2$, 25 mM HEPES, 10 mM glucose, 200 µM glutamate (pH adjusted to 7.4). Tetrodotoxin (TTX) 500 nM, 100 µM $CdCl_2$, 20 µM 6-cyano-7-nitroquinoxaline-2,3-dione (CNQX), 20 µM bicuculline, and 20 µM 2-amino-5-phosphonopentanoic acid (AP5) were added to the glutamate puffing and bath solutions to reduce neuronal excitability. For all puffing experiments, the puffer pipette was placed in the same focal plane as the voltage clamped cell and manipulated until a maximal response was elicited. All traces shown are the average of 3-4 consecutive applications of potassium or glutamate.

Immunoblotting

Following spinal cord extraction as described above, protein lysates were prepared by homogenization in lysis buffer (1% sodium dodecyl sulfate (SDS), 100 mM Tris(hydroxymethyl)aminomethane (Tris) buffer, pH 7.5, supplemented with protease and phosphatase inhibitors (Sigma)), using glass dounce homogenizers, followed by 2 rounds of sonication for 10 seconds. Lysates were spun at 12,000 g for 5 minutes at 4°C. Protein concentration of supernatant was determined by bicinchoninic acid (BCA) assay (Thermo Scientific). Protein was heated to 60°C for 15 min in an equal volume of 2× loading buffer (100 mM Tris, pH 6.8, 4% SDS, in Laemmli-sodium dodecyl sulfate, 600

mM β- mercaptoethanol, 200 mM dithiothreitol (DTT), and 20% glycerol). Equal amounts (10 µg) of protein were loaded into each lane of a 4 –20% gradient precast SDS polyacrylamide gel (Bio-Rad). Gels were transferred onto PVDF membrane (Millipore) at 100V for one hour. Membranes were blocked in blocking buffer (10% dried milk in Tris-buffered saline and Tween 20, (TBST) which contained 50 mM Tris, 150 mM NaCl, 0.05% Tween 20, pH adjusted to 7.4 with HCl). Blots were incubated with Kir4.1 (Alomone #APC-035) primary antibody 1:750 in blocking buffer at room temperature for 90 minutes. The membrane was then rinsed 3× for 15 min and incubated with horseradish peroxidase-conjugated anti-rabbit secondary antibody (Santa Cruz #SC2054, 1:2000) for 60 min at room temperature. After three 10 min washes, membranes were developed with Millipore Luminata Classic Western horseradish peroxidase substrate for visualization on CL-XPosure autoradiography film (Thermo Scientific). The blots were then stripped with Restore Stripping Buffer (Thermo Scientific) and re-probed with GLT-1 (Millipore #AB1783, 1:10 000), GFAP (Millipore #MAB5628, 1:30,000), and glyceraldehyde 3-phosphate dehydrogenase (GAPDH) (Millipore #AB2302, 1:1000) for a loading control, and Millipore anti-guinea pig (#AP108P), Santa Cruz anti-mouse (#SC-2005), and anti-chicken (#SC-2901) secondary antibodies at 1:2000. Protein expression was quantitated using ImageJ software, normalizing total GFAP, Kir4.1, or GLT-1 protein to GAPDH expression in the same lane.

Immunocytochemistry

Animals were anaesthetized with a peritoneal injection of ketamine (100mg/kg) and perfused with 4% paraformaldehyde solution for 25 minutes. The spinal cord was

removed and stored in 4% paraformaldehyde overnight at 4°C. After washing in PBS, 100µM sections were cut using a Vibratome (Oxford instruments). Sections were blocked for 1h in 10% goat serum and 0.2% Triton-X100 in phosphate buffered saline (BB). Following blocking, antibody incubation and washes were carried out in BB diluted 1:3 in PBS (diluted BB). Slices were incubated in primary antibody (GFAP, Dako #Z0334, 1:1000), (Kir4.1, Proteintech #12503-1-AP, 1:500), (GLT-1, Millipore #AB1783 1:1000), & (NeuN, Millipore #MAB377 1:1000) in diluted BB overnight at 4ºC with gentle agitation. The sections were then washed three times in diluted BB and incubated for 60 minutes at room temperature with tetramethyl rhodamine iso-thiocyanate-conjugated secondary antibodies obtained from Invitrogen (#A11008, #A11029, #A11010, #A11074) 1:500 in diluted blocking buffer. The slices were washed two times with diluted BB, then incubated with 4'6-diamidino-2-phenylindole (DAPI) 0.1µg/mL; (Sigma), and finally washed twice with phosphate buffered saline before being mounted onto glass coverslips. Fluorescent images were acquired with a Zeiss Axio Observer D1.

Quantitative Real-Time PCR

Following tissue removal as described above, for quantitative real-time polymerase chain reaction (qRT PCR), sequential isolation of total mRNA and genomic DNA were performed using Qiagen All Prep DNA/RNA Mini Kit. A total of 1.0µg of mRNA was converted to cDNA using Invitrogen Superscript VILO cDNA synthesis kit. Prior to PCR, cDNA was diluted 1:3 using DEPC treated water. Applied Biosystems Taqman probes were used with Taqman Universal Mastermix II, no UNG. An Applied Biosystems StepOne machine was used to perform qPCR and corresponding software

was subsequently used for analysis of results. Cycling parameters were: 50°C for 2 min, 95°C for 10 min, 40 repeats of 95°C for 15 s and 60°C for 1 min. *GAPDH* was used as control housekeeping gene. ΔΔCt method was used to determine relative fold expression of mRNA.

Cultured spinal cord astrocytes

For culture experiments, newborn (PND0) pups were decapitated. Spinal cords were removed and dissected in ice-cold serum-free EMEM (Gibco, Grand Island, NY) containing 20 mM glucose. Meninges were stripped and cords were minced and placed into O_2-saturated EMEM with papain (Worthington, Lakewood, NJ) for 20 min. Tissue was washed twice with spinal cord astrocyte media (EMEM supplemented with 10% fetal calf serum (FCS), 20 mM glucose, and penicillin/streptomycin) and triturated. Cells were plated at a density of 1.0×10^6 cells/ml on polyornithine- and laminin-coated 12-well tissue culture plates (Falcon). The media was changed the first and second days, and every fourth day thereafter. Mature or differentiated spinal cord astrocytes (>6 days in culture [DIC]) were used for all cultured experiments.

shRNA treatment

E.coli containing shRNA sequence targeted for GFAP, GE Healthcare Dharmacon shRNA construct #TRC0000090606, were cultured overnight at 37ºC on LB agar plates supplemented with 100µg/ml carbenicillin. A single colony was added to 10ml LB broth with carbenicillin and incubated overnight at 37ºC. shRNA was isolated using a QIAprep Spin Miniprep kit. GFAP shRNA treatment occurred at 10DIC using

Lipofectamine transfection reagent (Invitrogen) and RNA was collected 24hr following treatment.

Statistical analysis

Current responses to varied voltage steps and ramps were analyzed and measured in Clampfit (Molecular Devices); the resulting raw data were graphed and plotted in Origin 8.51 (MicroCal). Two-tailed t-test, Tukey-Kramer Multiple Comparisons Test, and Mann-Whitney tests were performed using Graphpad software (San Diego, CA) and P values are reported in the text. Unless otherwise stated, all values are reported as means ± SE with n indicating the number of cells sampled.

RESULTS

Elevated GFAP induces gliotic reduction of Kir4.1 and GLT-1 expression in AxD mouse models

To investigate the possibility that alterations in Kir4.1 and GLT-1 functions in caudal brain regions have a role in type II AxD, we first examined Kir4.1 and GLT-1 protein expression in caudal brain regions from three animal models of AxD: a line in which wild type (WT) human GFAP is overexpressed from a transgene ($hGFAP^{TG}$, Messing et al., 1998); a line heterozygous for an R236H knock-in mutation, which is homologous to the common and particularly severe R239H mutation in human patients ($R236H^{+/-}$ Hagemann et al., 2006); and mice generated by crossing these two lines, ($hGFAP^{TG}/R236H^{+/-}$ Hagemann et al., 2006). Both the $hGFAP^{TG}$ and $R236H^{+/-}$ mice have elevated GFAP expression in hippocampus and cortex, form Rosenthal fibers, display CNS oxidative stress and are hypersensitive to kainic acid induced seizures, but have a normal lifespan and no myelin deficits. The same observations hold for $hGFAP^{TG}/R236H^{+/-}$ mice (Hagemann et al., 2006), except that the changes occur sooner, are more severe, and these mice die by 35 days of age from seizures (Hagemann et al., 2006). We have also observed a full body clasp when these mice were suspended by the tail in the days prior to death (unpublished observations), suggesting profound motor impairment (Yamamoto et al., 2000;Mangiarini et al., 1996;Filali et al., 2011). Additionally, $hGFAP^{TG}$ animals have significantly lower body weight and increased

brain water volume (Meisingset et al., 2010), and both hGFAP^{TG} and R236H$^{+/-}$ animals display higher susceptibility to kainic acid induced seizures than their wild-type littermates (Eng et al., 1998;Hagemann et al., 2006). However, the absence of myelin deficits in these mice suggests they better model late onset, type II AxD, than the type I form.

Astrocytic proteins Kir4.1, GLT-1, and GFAP were quantified in the three models of AxD with GAPDH as a loading control (Fig. 7). At four weeks of age significant increases in GFAP were present in both hGFAP^{TG} (72.3 ± 6.0%) and hGFAP^{TG}/R236H$^{+/-}$ (36.7 ± 4.4%) in cervical spinal cord, but no significant change in GFAP amount was detected from R236H$^{+/-}$ animals relative to WT. Corresponding with the upregulation of GFAP, hGFAP^{TG} animals demonstrated significantly lower amounts of Kir4.1 (~75% reduction) and GLT-1 (~60% reduction) and the double transgenic hGFAP^{TG}/R236H$^{+/-}$ animals exhibited a near complete loss of Kir4.1 and GLT-1 immunoreactivity. This is despite the fact that the increase of GFAP expression in these animals was less than that in the hGFAP^{TG} mice, indicating that the R236H mutation contributes to the molecular changes observed in hGFAP^{TG}/R236H$^{+/-}$ mice. Of note, we and others have shown multiple bands on Kir4.1 Western blots that correspond with a monomer through tetramer (~50 kD – 200 kD) of the Kir4.1 protein (Kaiser et al., 2006;Olsen et al., 2010b). These bands are completely absent in Kir4.1 KO animals and in human embryonic kidney cells that do not express Kir4.1 (Olsen et al., 2006). Therefore, the entire lane is used for quantitation. The image shown for the Kir4.1 western blot has been overexposed to indicate the striking loss of Kir4.1 in hGFAP^{TG}/R236H$^{+/-}$ animals compared to WT animals; non-saturated exposure images were used for quantitation. In contrast, R236H$^{+/-}$

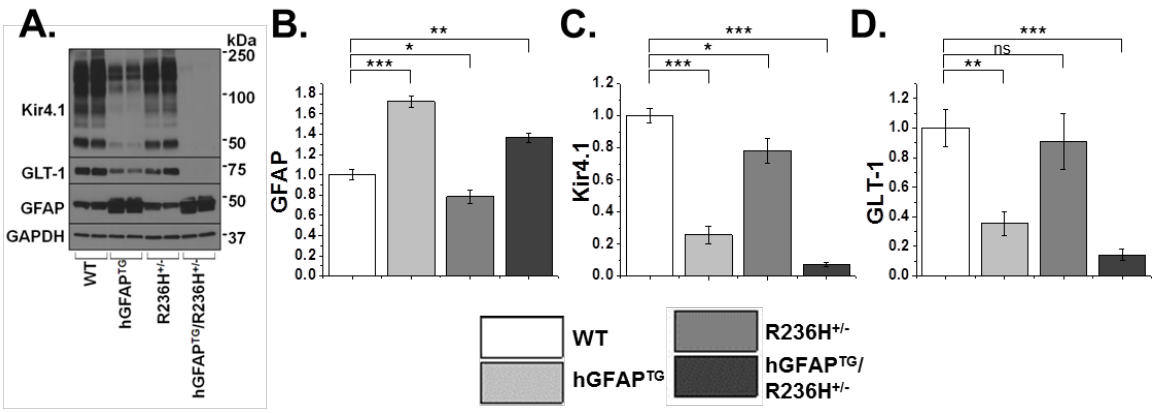

Figure 7. Kir4.1 and GLT-1 protein expression are reduced in spinal cord of AxD mice.

A. Western blot analysis of spinal cord from PND 24-28 WT, hGFAP^{TG}, R236H$^{+/-}$, and hGFAP^{TG} /R236H$^{+/-}$ mice for Kir4.1, GLT-1 and GFAP and for GAPDH as a loading control are shown. **B-D.** Quantification of western blot in (A) for GFAP (**B**), Kir4.1 (**C**), and GLT-1 (**D**), normalized to GAPDH levels and WT values are shown. Data are ± SEM, n=4 in all groups, unpaired t-tests, *=p<0.05, **=p<0.01, ***=p<0.001.

R236H$^{+/-}$ animals demonstrated no increase in GFAP protein (Fig. 7A,B) at the four-week time point compared to WT animals. A slight but significant reduction in Kir4.1 protein was observed in R236H$^{+/-}$ spinal cord (Fig. 7A,C), but no significant differences in GLT-1 immunoreactivity were observed (Fig.7A,D). Because pathological changes increase with time in these mice, we also examined R236H$^{+/-}$ animals at two months and one year of age, but found no change in GFAP (data not shown). It is important to note that these observations are specifically for brainstem and spinal cord, as elevated GFAP expression and Rosenthal fiber accumulation is observed in the hippocampus of R236H$^{+/-}$ animals (Hagemann et al., 2006). Given no increase in GFAP in the spinal cord and brainstem in R236H$^{+/-}$, we chose to omit these animals from the remainder of the study. Additionally, the early lethality of the double hGFAP^{TG}/R236H$^{+/-}$ transgenic mice represents a severe form of AxD not representative of the later onset type II AxD. Therefore we focused on the hGFAP^{TG} model in subsequent experiments as an appropriate model of type II AxD.

Mature astrocytic protein expression profiles are established by four weeks of age in wild type mice, with GFAP, Kir4.1 and GLT-1 mRNA upregulated during early postnatal development in all CNS regions. Figure 8 demonstrates normal transcript increases measured by quantitative PCR (qPCR) over the first two postnatal weeks in wild type spinal cord tissue, and corresponding increases in protein by Western blot detection. Each of these three genes is rapidly induced throughout this time, with GFAP and GLT-1 transcripts effectively doubling from PND3 to 7, and again between 7 and 14 days of age (Fig.8A). Kir4.1 mRNA levels increase about four-fold in the four days

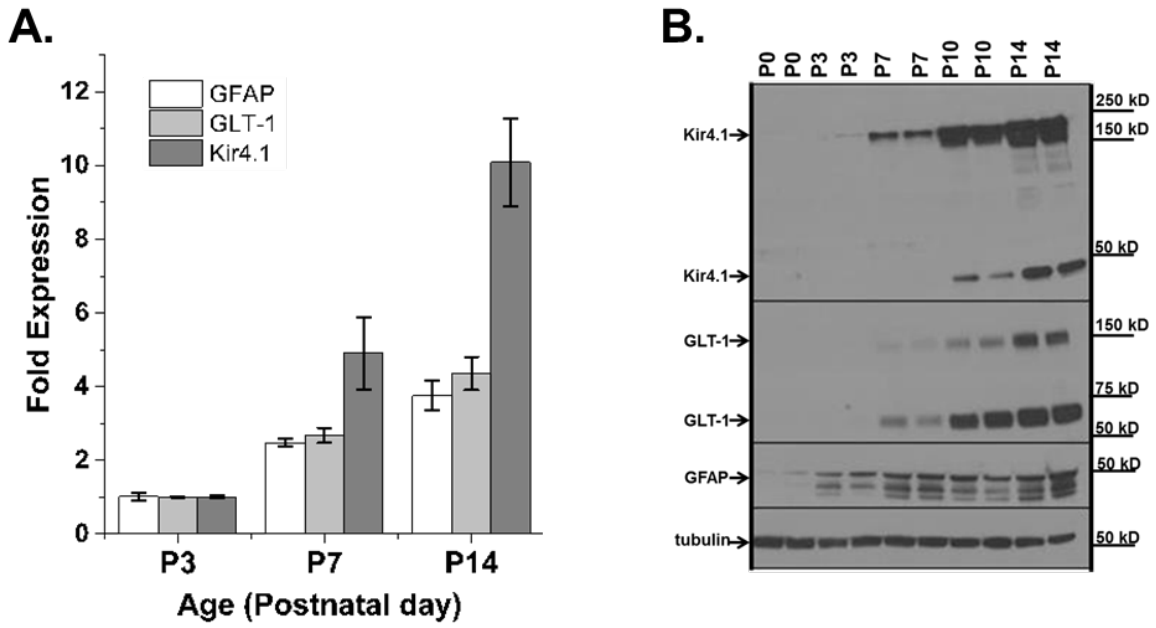

Figure 8. Expression of key astrocytic genes is developmentally regulated.

A. Quantitative PCR demonstrates increased transcript levels of *GFAP, SLC1A2, and KCNJ10* through two weeks of age in WT mouse spinal cord. Quantitative PCR data are shown relative to *GAPDH* expression and normalized to P3 samples. **B.** Western blot analysis of WT spinal cord ranging in age from postnatal day 0-14 demonstrates induction of protein expression correlated to transcript levels for GFAP, GLT-1, and Kir4.1 during the first two weeks of postnatal development, with tubulin shown as a loading control.

between PND3 and 7, and are around 10 times greater in PND14 spinal cord tissue than at PND3. The dramatic upregulation of each of these genes is mirrored by changes in protein expression during the same developmental time points, indicating a tight correlation between mRNA and protein expression for each gene (Fig.8B).

Given this dramatic change in expression across this short developmental period, we sought to better understand the consequences of GFAP overexpression during this critical developmental period. We examined *GFAP* expression in WT and hGFAP^{TG} spinal cord throughout this critical temporal window of astrocyic differentiation and maturation. QPCR analysis demonstrates that endogenous GFAP transcript levels in the spinal cord of hGFAP^{TG} animals are similar to WT littermate controls at PND 3 and PND 7 and became significantly increased by PND 14 (~70%, Fig. 9A). A similar pattern of time-dependent expression exists for human *GFAP* (hGFAP) transcript levels that also steadily increase over the first 14 postnatal days in hGFAP^{TG} spinal cord (Fig, 9B). Together with endogenous GFAP, the presence of human GFAP accelerates total GFAP protein accumulation in spinal cord tissue. Western blot of spinal cord tissue from WT and hGFAP^{TG} littermates at PND7 demonstrates that total GFAP levels, as detected by a non-species specific antibody, are dramatically increased at PND7 (Fig. 9C). Kir4.1 immunoreactivity is also decreased, while GLT-1 appears similar to WT at 7 days of age. At the mRNA level, however, expression of both Kir.1 and GLT-1 are reduced at P7 (Figs. 9D,9E), suggesting a transcriptional mechanism of regulation associated with a 'gliotic' phenotype rather than a post-translational mechanism.

We next queried whether the decreased Kir4.1 and GLT-1 protein in hGFAP^{TG} mice was autonomous to the astrocyte or secondary to the disease process occurring in

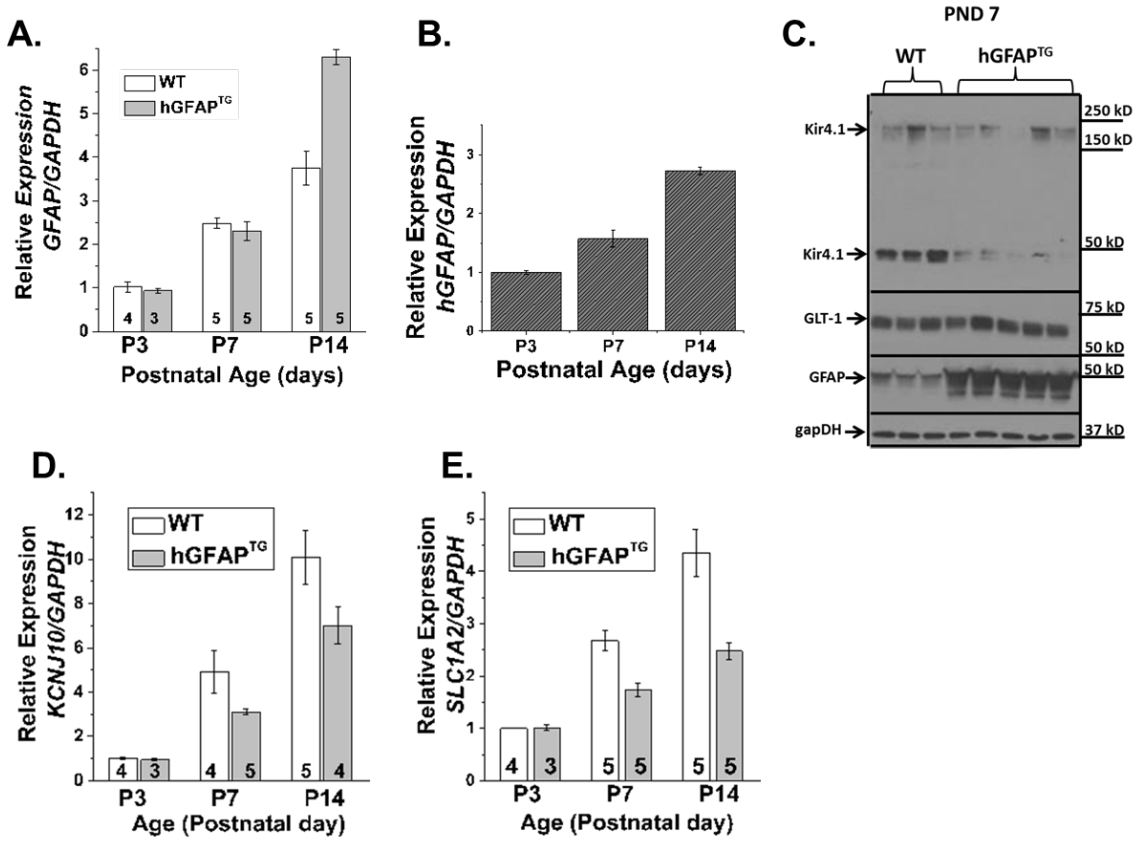

Figure 9. *hGFAP* contributes to GFAP protein accumulation and early developmental reductions in Kir4.1 and GLT-1 mRNA expression in hGFAP^{TG} spinal cord.

A. Quantitative PCR demonstrates upregulation of endogenous mouse GFAP between PND7 and 14. **B.** Transcript for *hGFAP* also gradually increases throughout this time **C.** Western blot of PND7 WT and hGFAP^{TG} spinal cord reveals hGFAP contributes to increased GFAP protein accumulation prior to differential induction of endogenous mouse GFAP transcript in hGFAP^{TG} spinal cord, which occurs between PND7-14. GAPDH is shown as loading control. QPCR for *KCNJ10* (**D.**) and *SLC1A2* (**E.**) demonstrates reduced transcript for Kir4.1and GLT-1 as early as PND7, correlating with increased GFAP protein accumulation present by this time. QPCR values are reported relative to *GAPDH* and normalized to PND3 WT, n=3-5.

these mice. This is an important question given the observations that GFAP is elevated in all CNS insults. To address this question, we cultured spinal cord astrocytes from WT and hGFAP^{TG} mice, thereby removing them from the context of the diseased brain. Western blot analysis from spinal cord astrocyte cultures collected 10-12 days after plating indicated reduced Kir4.1 protein in hGFAP^{TG} mice relative to astrocyte cultures from WT littermates (Figure 10A). Similar results were observed for GLT-1 (Fig. 10B). These data coupled with the previous experiments demonstrate that elevated GFAP expression is sufficient to induce significant reductions of Kir4.1 and GLT-1 protein and mRNA transcripts in a cell-automomous manner.

To determine if the differences in Kir4.1 and GLT-1 in the hGFAP^{TG} mice was transitory or of long duration, we examined protein expression in mice ranging in age from 14 days to 11 months (Fig. 11). Because both brainstem and spinal cord function are affected in Type II AxD, we examined tissue from both structures. Brainstem and spinal cord demonstrated a reduction in Kir4.1 and GLT-1 protein (Fig. 11A) and mRNA (Fig. 11B) expression at PND 14, a time where these proteins normally begin to peak (Jany et al., 2013; Nwaobi et al., 2014). Furthermore, Western blot analysis from brainstem and spinal cord tissue indicated that these effects are maintained throughout adulthood (Fig. 11C). Together, these data demonstrate significant alterations in Kir4.1 and GLT-1 mRNA and protein in both spinal cord and brainstem associated with elevated GFAP expression in hGFAP^{TG} mice occur early in postnatal development and persist through adulthood.

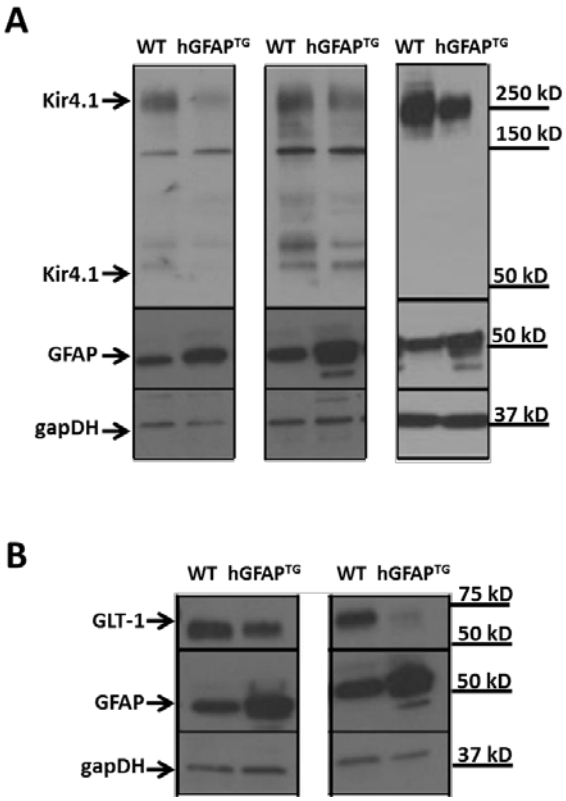

Figure 10. Cultured hGFAP^{TG} astrocytes develop increased GFAP and decreased GLT-1 and Kir4.1 proteins *in vitro*

Western blot analysis of independent primary astrocytic cultures obtained from WT and hGFAP^{TG} PND0 spinal cord comparing GFAP, Kir4.1 (**A.**), and GLT-1 (**B.**) expression 10-12 days *in vitro.* GAPDH is shown as a loading control.

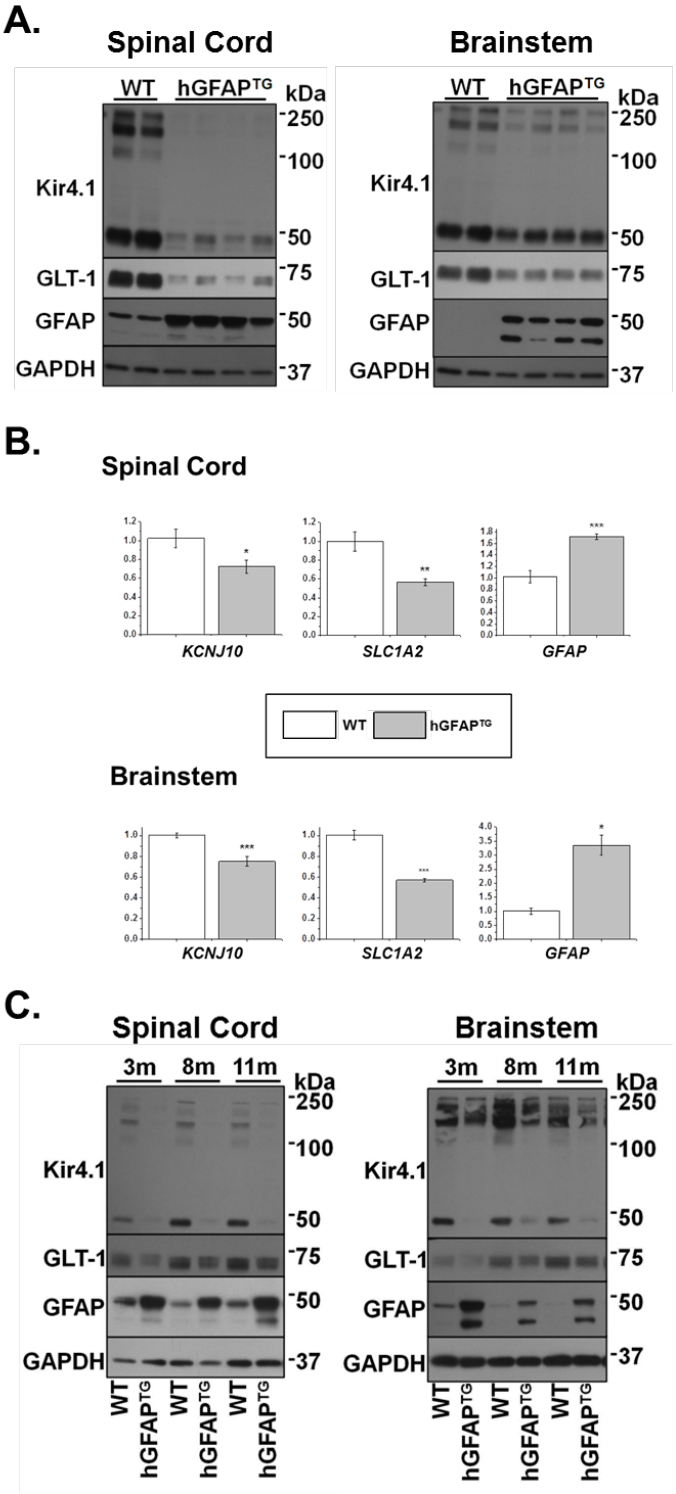
A.
Spinal Cord
Brainstem
WT
hGFAP^TG
kDa
250
100
50
75
50
37
Kir4.1
GLT-1
GFAP
GAPDH
B.
Spinal Cord
KCNJ10
SLC1A2
GFAP
WT
hGFAP^TG
Brainstem
C.
Spinal Cord
Brainstem
3m
8m
11m
WT
hGFAP^TG

Figure 11. Protein and mRNA alterations in hGFAP^{TG} mice are consistent in brainstem and spinal cord, and persist from development through adulthood. **A.** Representative Western blots for Kir4.1, GLT-1, and GFAP protein expression in PND14 cervical spinal cord and brainstem are shown. Data includes 4 hGFAP^{TG} mice and 2 littermate controls. **B.** QPCR of PND14 mice demonstrate transcript expression paralleling protein observed in (A) including reductions in *KCNJ10* and *SLC1A2* in both spinal cord and brainstem tissues, while *GFAP* transcript is elevated in the same tissues of hGFAP^{TG} mice compared to WT littermates. **C.** Western blot analyses of spinal cord and brainstem from 3, 8, and 11 month old hGFAP^{TG} mice and WT littermates are shown for Kir4.1, GLT-1 and GFAP, and for GAPDH as a loading control. In brainstem, exposures were minimized to prevent saturation of GFAP signal in mutant animals.

To assess the spatial distribution of astrocytic changes within the spinal cord, immunohistochemistry analysis of 1-month old wild type and hGFAP^{TG} spinal cords was performed for GFAP, Kir4.1, and GLT-1 proteins (Fig. 12). We and others have shown that Kir4.1 and GLT-1 expression is most highly expressed in the gray matter neuropil and largely demarcates gray matter from white matter in transverse spinal cord sections (Olsen et al., 2007). Here we observed a similar pattern of expression of Kir4.1 and GLT-1 expression in four week old WT mice (Fig. 12). Kir4.1 immunoreactivity was markedly reduced throughout the gray matter in transverse spinal cord sections from hGFAP^{TG} mice relative to WT littermates. These differences are observed in low magnification images that enable visualization of the entire transverse section (left panels) and at higher magnification of the ventral horn (right panels). GFAP immunoreactivity was elevated throughout each transverse section, particularly in gray matter and subpial white matter. A similar pattern of loss was observed across spinal cord and in the ventral horn for GLT-1 immunoreactivity (Fig. 12C,D). The loss of Kir4.1 and GLT-1 as well as the increase in GFAP expression was observed throughout cervical and lumbar regions of the spinal cord. The decrease of Kir4.1 and GLT-1 protein surrounding motor neurons in cervical spinal cord may provide a mechanism by which astrocytes contribute to hindbrain symptoms in type II AxD.

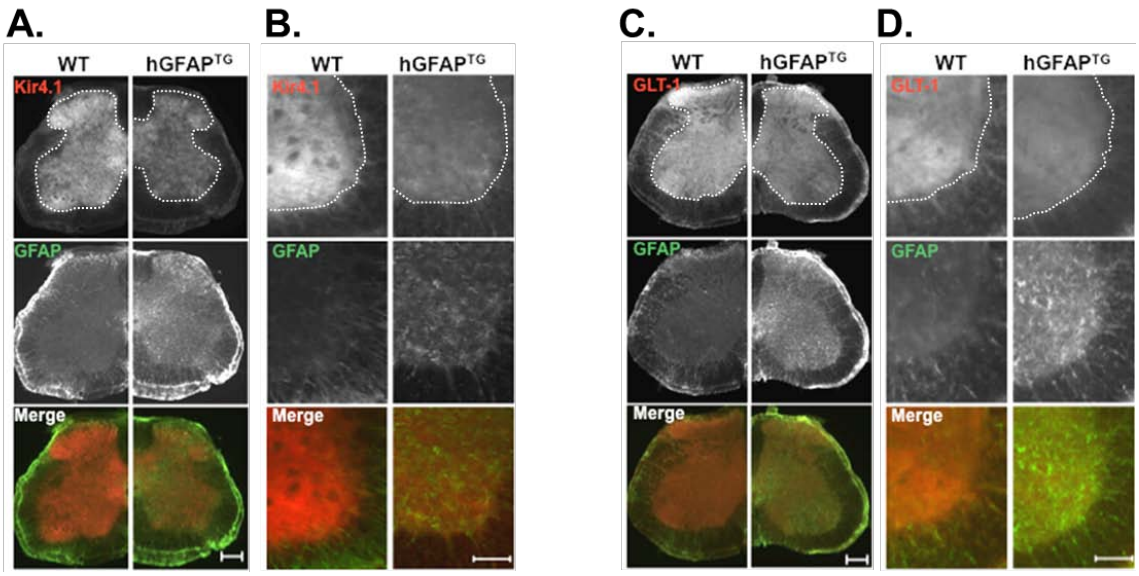

Figure 12. Immunohistochemistry from transverse spinal cord sections demonstrates loss of Kir4.1 and GLT-1 in PND 28 hGFAP^{TG} mice relative to WT littermates.

A. Low magnification (5X) images from transverse spinal cord sections indicate decreased Kir4.1 expression throughout the gray matter in hGFAP^{TG} mice (*top panel*). GFAP is elevated in hGFAP^{TG} sections (*middle panel*). Visualized together in the merged image, the loss of Kir4.1 (red) and increased GFAP (green) are apparent. **B.** As shown in A, higher magnification (20X) demonstrates protein changes in ventral horn. **C.** Low magnification (5X) images from transverse spinal cord sections indicate decreased GLT-1 expression throughout the gray matter in hGFAP^{TG} mice (*top panel*). GFAP is elevated in hGFAP^{TG} sections (*middle panel*). Visualized together in the merged image, the loss of GLT-1 (red) and increased GFAP (green) are apparent. **D.** As shown in C, higher magnification (20X) demonstrates protein changes in ventral horn. Dotted line demarcates gray from white matter. Scale bars (A,C = 200 µm, B,D = 100 µm).

hGFAP^{TG} spinal cord astrocytes exhibit decreased Kir4.1 currents and reduced K^+ uptake

A primary cause of death in type II AxD patients is aspiration pneumonia due to dysphagia or an inability to swallow properly (Pareyson et al., 2008). This and other hindbrain symptoms in patients with type II AxD indicate profound motor dysfunction in cervical spinal cord regions. To better understand the implications of the loss of Kir4.1 and GLT-1 and their possible contribution to disease development, we assessed the capacity of cervical ventral horn astrocytes to perform their normal, neuronal supportive function of potassium regulation.

Whole-cell, electrophysiological recordings were performed from ventral horn astrocytes in acute cervical spinal cord sections from PND 14-18 WT and hGFAP^{TG} animals. Astrocytes were visually identified based on morphology and electrophysiological properties. In some experiments, electrophysiological recordings were performed in hGFAP^{TG} animals crossed with ALDH1L1-EGFP mice (green astrocytes) to assist with visualization (Yang et al., 2011). To activate Kir4.1 currents, we stepped astrocytes from -80 mV to 0 mV for 100 ms, and then from -180 to 100 mV in 20 mV increments as previously described (Olsen et al., 2007). Barium chloride ($BaCl_2$, 100 μM) was used to isolate currents mediated by Kir4.1 channels as previously described (Ransom and Sontheimer, 1995). The resulting subtracted currents were identified as Kir4.1 currents. As depicted in Figure 13A, Ba^{2+}-sensitive Kir4.1 currents were markedly smaller in hGFAP^{TG} astrocytes. Indeed the whole cell currents in hGFAP^{TG} animals were very similar to the post-Ba^{2+} trace in WT animals. A current-voltage (I-V) plot derived from voltage steps such as shown in Figure 13A indicates significant

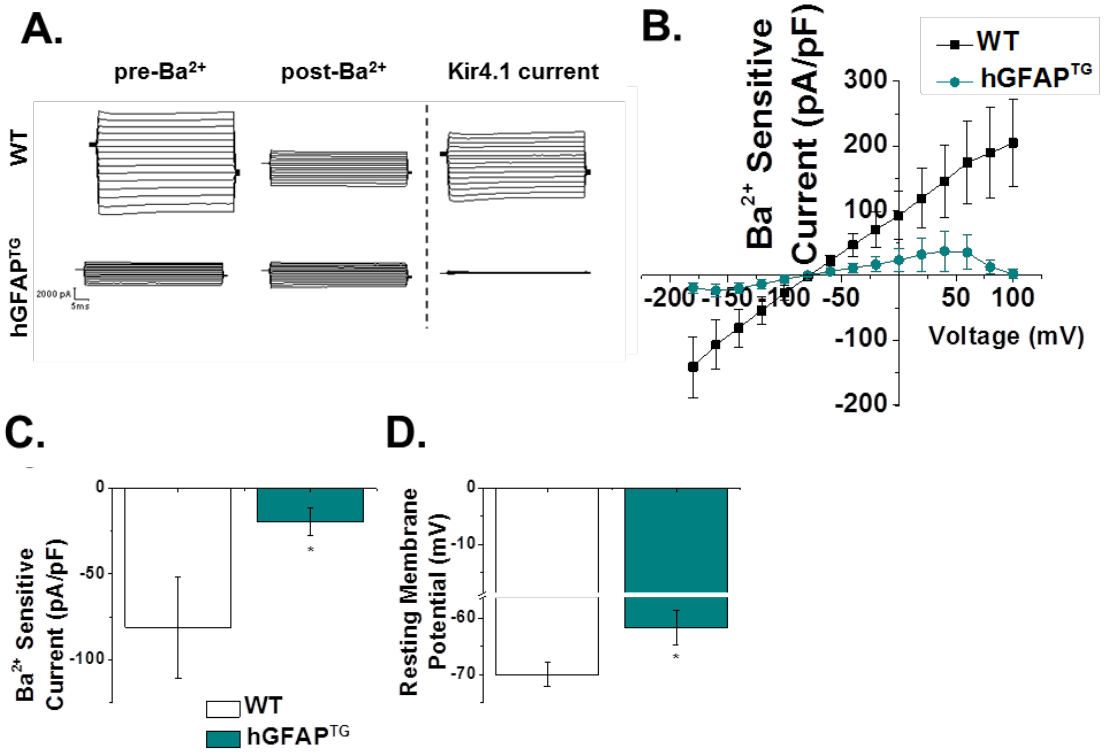

Figure 13. Kir4.1-mediated currents are smaller and astrocyte intrinsic membrane properties are altered in hGFAP^{TG} mice compared to WT littermates.

A. Representative whole-cell recordings in response to a voltage-step protocol demonstrate a significant decrease in current amplitude in hGFAP^{TG} ventral spinal cord astrocytes. **B.** I-V plot of cumulative data obtained from Ba^{2+}-sensitive subtractions normalized to whole-cell capacitance demonstrates both diminished inward and outward currents in hGFAP^{TG} astrocytes. **C.** Current density is significantly decreased at -140 mV in hGFAP^{TG} astrocytes (WT, -81 ± 30 [n=14] hGFAP^{TG}, -17 ± 8 pA/pF, [n=10], Mann-Whitney Test, p= 0.0158). **D.** The mean resting membrane potential of astrocytes is significantly depolarized in hGFAP^{TG} mice relative to WT littermates (WT, -70 ± 2mV [n = 16]; hGFAP^{TG}, -62 ± 3 mV [n = 14]; two-tailed t-test, p= 0.0302).

differences between WT and hGFAP^{TG} Ba^{2+}-sensitive, Kir4.1-mediated currents (Fig. 13B). This is represented graphically at one potential (-140 mV) in Figure 13C, which shows a change in current density from -81 ± 30 in the WT to -17 ± 8 pA/pF in the hGFAP^{TG} mice. Astrocytes from hGFAP^{TG} animals were also significantly depolarized (-62 ± 3 mV) relative to WT littermates (-70 ± 2 mV, Fig. 13D).

To more directly measure the effects of reduced Kir4.1 on potassium uptake by hGFAP^{TG} astrocytes, we applied 30 mM K^+ for 400 ms using a picospritzer to mimic focal increases in $[K^+]_o$ as would occur following neuronal activity. The puffer pipette was placed in the same focal plane as the voltage clamped cell at a distance that elicited a maximum response. Recordings were obtained from ventral horn astrocytes voltage-clamped at -80 mV. For clarity we show the response from each WT and hGFAP^{TG} astrocyte (Fig. 14A). Mean data are summarized in Figure 14B. A scatter plot of peak current amplitudes in response to a potassium puff demonstrates a significant reduction in the overall amplitude of the K^+ puff response in hGFAP^{TG} astrocytes (-218 ± 44 pA) relative to astrocytes from WT littermates (-645 ± 15.4 pA). The variability in the scatter plot values for the WT animals may result from the recordings being performed between PND 14-18, the time when Kir4.1 expression increases most dramatically (Nwaobi et al., 2014), and thus likely would vary among cells. In contrast, there is little variability among the hGFAP^{TG} cells, presumably because their Kir4.1 levels remain uniformly low. These data indicate reduced capacity for potassium uptake consistent with the Kir4.1 protein loss indicated by Western blot.

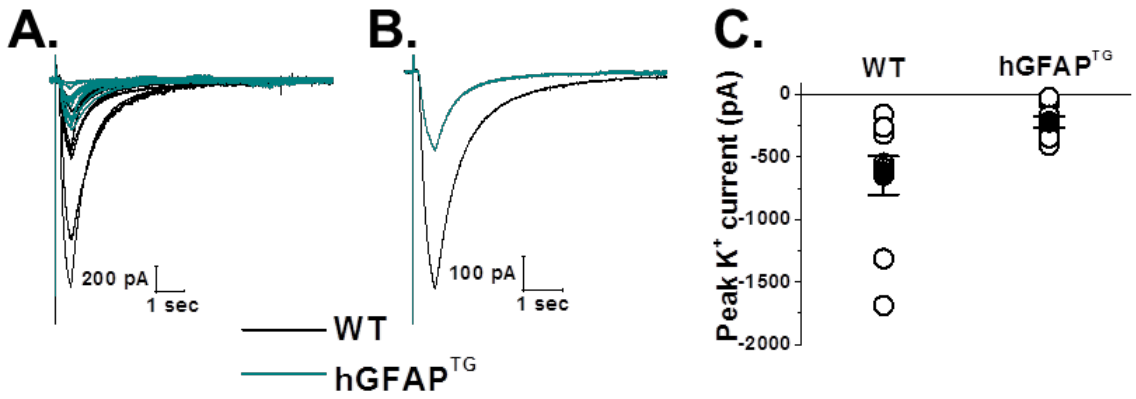

Figure 14. $[K^+]_o$ uptake by ventral spinal cord astrocytes is decreased in hGFAP^{TG} mice relative to WT littermates.

A. Superimposed traces of WT (black, n = 9) and hGFAP^{TG} (cyan, n = 8) potassium currents in response to application of a brief (400 ms) application of 30mM potassium are indicated. **B.** Averaged traces from A are shown. **C.** Peak amplitudes of individual cells (open circles) from A and mean data (filled circles) indicate a significant decrease in potassium uptake in hGFAP^{TG} mice (WT,-645 ± 15 [n= 9]; hGFAP^{TG}, -218 ± 44 [n = 8], two tailed t-test, p = 0.0264).

Whole-cell glutamate transporter currents are reduced in hGFAP^{TG} spinal cord astrocytes in response to glutamate challenge

We next examined the response of astrocytes from the ventral horn to exogenously applied glutamate. To isolate glutamate transporter currents and minimize neuronal activity and release of endogenous glutamate we included 500 nM TTX, 100 µM $CdCl_2$, 20 µM CNQX, 20 µM bicuculline and 20 µM AP5 in both the bathing solution and the glutamate puffing pipette (Bergles and Jahr, 1997;Grass et al., 2004). Using a picospritzer we pressure applied glutamate (200 µM, 400 ms) to ventral horn astrocytes voltage clamped at -80 mV. As with the K^+ puffing experiments, the puffing pipette was manipulated until the maximum response was elicited from the voltage clamped cell. The resulting traces from 15 WT and 9 hGFAP^{TG} astrocytes are shown in Figure 15A. Averaged data from all WT and hGFAP^{TG} astrocytes are shown in Figure 15B. The summary scatter plot demonstrates a significant decrease in the glutamate uptake currents in response to a challenge of glutamate in ventral horn hGFAP^{TG} astrocytes (-8.1 ± 4.1pA) relative to WT astrocytes (-53.2 ± 4.1 pA). Taken together, these data demonstrate altered astrocyte biophysical properties and reduced capacity to clear glutamate and K^+ in a model of type II AxD. This loss correlates with reduced levels of both Kir4.1 and GLT-1 proteins. We propose that these changes in astrocyte physiology contribute to hindbrain pathology and symptoms in type II AxD.

Kir4.1 protein expression profiles vary between areas affected in type I vs. type II AxD

While our study was in progress, Sosunov et al. (2013) published the observation that Kir4.1 levels were increased in the hippocampus of hGFAP^{TG} mice, contrary to our

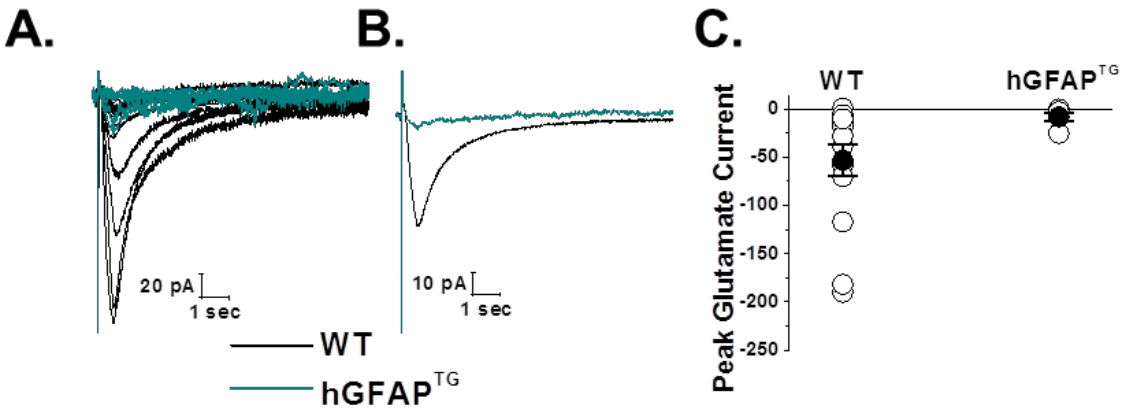

Figure 15. Glutamate uptake in ventral spinal cord astrocytes is reduced in hGFAP^{TG} mice compared to WT littermates.

A. Superimposed traces of glutamate transporter currents recorded from ventral horn astrocytes from WT (black, n = 15) and hGFAP^{TG} (cyan, n = 9) astrocytes are shown. Cells were voltage clamped at -80 mV and responses were evoked by a 200 µM, 400 ms puff of glutamate. Bathing and puffing solutions contained 20 µM AP5, 20 µM bicuculline, 20 µM CNQX, 500 nM TTX and 100 µM $CdCl_2$. Each trace shown is an average of three individual traces for that astrocyte. **B.** Averaged data across all WT (black) and hGFAP^{TG} (cyan) responses are shown. **C.** Summary scatter plot of the glutamate evoked responses indicates a decrease in the hGFAP^{TG} mice (-8.1 ± 4.1 pA [n = 9]) relative to WT littermate controls (-53.2 ± 4.1 pA [n = 15], two tailed t-test, p = 0.0416).

report here of a marked decrease in brainstem and spinal cord. To determine if the change in Kir4.1 levels was indeed CNS region specific, we performed Western blots for Kir4.1 and GLT-1 for hippocampal and cortical tissues isolated from 3, 8, and 11 month old $hGFAP^{TG}$ mice and WT littermates. As shown in Figure 16, we confirm the report of (Sosunov et al., 2013), of an increase of Kir4.1 levels in the hippocampus, as well as their finding of a decrease in GLT-1. It is unclear why Kir4.1 expression is so differently and dramatically affected along the rostro-caudal axis in $hGFAP^{TG}$ mice; this may reflect regional astrocyte heterogeneity.

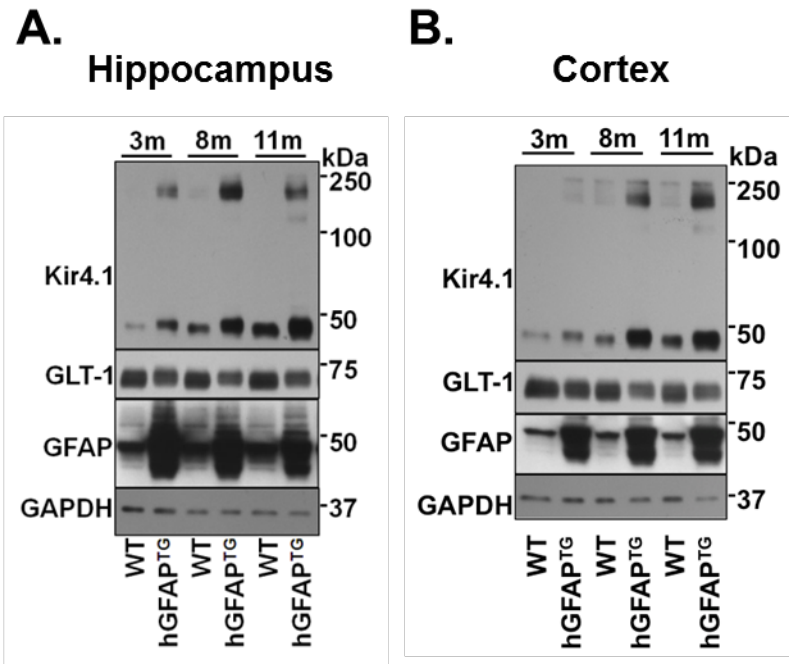

Figure 16. Kir4.1 and GLT-1 protein expression in hippocampus and cortex of hGFAP^{TG} differ from caudal brain regions.

Western blot of hippocampus (**A**) and cortex (**B**) from 3, 8, and 11-month-old hGFAP^{TG} mice and WT littermates for Kir4.1, GLT-1 and GFAP, and for GAPDH as a loading control are shown.

SUMMARY AND DISCUSSION

Significant progress has been made over the last two decades defining the critical roles astrocytes play in 'normal' CNS functioning and how they contribute to disease processes. Reactive astrocytes or astrocytes associated with a diseased or injured brain demonstrate a broad spectrum of structural, protein and mRNA changes. One consistent observation that presents regardless of the context of the disease or injury is increased GFAP expression; which typically is more pronounced as disease progresses or as the severity of the insult increases. Although the role of GFAP in the gliotic astrocyte has yet to be determined, the commonality of this finding hints at its' significance. In this thesis, I explore the relationship between elevated GFAP expression in an animal model of AxD and fundamental homeostatic processes of K^+ and glutamate regulation. Here we show that Kir4.1 and GLT-1, which mediate the processes of K^+ and glutamate uptake, are dysregulated in the spinal cord and brainstem of AxD mice. This dysregulation is a result of significantly reduced protein levels, which manifest as early as PND 7-14 (the earliest time points examined) and persist through adulthood. The reductions in Kir4.1 and GLT-1 expression appear directly related to elevated GFAP expression as the reductions are not observed in an AxD model that carries a mutation but does not overexpress GFAP in caudal brain regions. We propose these changes in astrocyte physiology contribute to hindbrain-involved pathology and symptoms in type II AxD and

may provide insight to other CNS diseases that demonstrate high levels of GFAP expression.

The role of Kir4.1 and GLT-1 in type II AxD

To our knowledge, this is the first study to examine astrocytes in hindbrain regions in animal models of AxD. Our data comparing three mouse lines indicate that increased GFAP is necessary to induce changes in expression of other astrocytic proteins. In the $hGFAP^{TG}$ line where reductions in Kir4.1 and GLT-1 proteins are seen, astrocytes display impaired abilities to uptake both K^+ and glutamate. As reviewed in the introduction, the importance of Kir4.1 and GLT-1 to 'normal' CNS functioning is supported from Kir4.1 and GLT-1 mouse knockout studies. In the absence of either protein, severe symptoms and fatality occur. It is interesting to note that GLT-1 knockout mice display seizures and hind limb clasping, a sign of motor impairment/motor degeneration, prior to death (Tanaka et al., 1997;Kiryk et al., 2008). Similarly, seizure, ataxia and hind limb splaying/paralysis are present in Kir4.1 knockout animals (Neusch et al., 2001;Djukic et al., 2007). This list of symptoms is closely related to those observed in AxD.Although $hGFAP^{TG}$ mice are "mild" over-expressers that do not result in early mortality, behavioral testing does indicate significant reductions in forepaw grip strength, a motor skill dependent on cervical spinal cord function (Meisingset et al., 2010). All of these findings suggest that dysfunction of astrocytic regulation of K^+ and glutamate results in similar pathology in the spinal cord, and in the case of AxD, loss of Kir4.1 and GLT-1 protein expression and function in this region may contribute to motor dysfunction observed in type II AxD.

The contribution of reduced GLT-1 and Kir4.1 proteins to pathology of type II AxD may be better understood by reviewing research in animal models of various CNS disorders also featuring severe gliosis. In both ALS and MS the relevance of GLT-1 protein loss to the progression of pathology is well established and therapeutic interventions resulting in increased GLT-1 expression have been tested in animal models of ALS and MS (Melzer et al., 2008; Benkler et al., 2013) and in human ALS patients (Berry et al., 2013). Similarly, identifying Kir4.1 associated pathology includes the discovery of antibodies against Kir4.1 in MS patient serum, identifying it as a direct target in a subset of patients (Srivastava et al., 2012). Indicating a causal role for Kir4.1 in disease pathogenesis, viral restoration of Kir4.1 specifically to astrocytes reversed cellular and behavioral phenotypes and prolonged survival in Huntington's disease mice (Tong et al., 2014). Indeed, these and similar findings between other caudal pathologies, including spinal cord injury and chronic pain, have prompted the exploration of astrocyte targeted therapeutics (Olsen et al., 2010; Ramos et al., 2010). For example, experimental use of Ceftriaxone, an antibiotic shown to increase GLT-1 expression and shown to be beneficial in models of SMA (Hedlund, 2011), ALS (Benkler et al., 2013), and MS (Melzer et al., 2008) have also been chronically administered to an individual with type II AxD. Clinically, Ceftriazone arrested disease progression and resulted in reversal of clinical symptoms, which was sustained over a four-year treatment period (Sechi et al., 2012). At this point, it is unclear if Ceftriazone also affects Kir4.1 expression. Although in initial stages of investigation, targeting astrocytic specific dysfunction or gliosis in general, may provide promising new therapeutic strategies.

GFAP in AxD and gliosis

Data both presented and reviewed here suggest teasing apart the contribution of individual protein changes to gliosis-associated pathology is difficult due to the complex protein interactions within astrocytes. One important relationship does appear to have clear directionality, and that is our data indicate that overexpression of GFAP is sufficient to prevent 'normal' levels of Kir4.1 and GLT-1 protein expression in at least some populations of astrocytes, in the absence of any other underlying disease mechanism or precipitating insult. The reverse appears to be true as well. The example of Ceftriaxone treatment resulting in increased GLT-1 expression also decreases reactive induction of GFAP in a number of CNS insults (Ramos et al., 2010). Similarly, estrogen receptor signaling at physiological levels also decreases gliosis (Martinez and de Lacalle, 2007), and blocks GFAP increases (Perez-Alvarez et al., 2012) associated with injury and disease. These data further demonstrate an inverse relationship between GFAP and Kir4.1/ GLT-1 expression. Importantly, we also demonstrate that this phenotype is maintained *in vitro* in pure astrocyte cultures, indicating this relationship is intrinsic to the astrocyte and is not dependent on neuronal-astrocyte interaction. GFAP does not appear to directly interact with Kir4.1 (Fort et al., 2008), or GLT-1 (Sullivan et al., 2007). However, as membrane-bound proteins, they may rely on proper filament formation for trafficking and localization, and disruption could lead to the observed decreased currents. Neither published reports nor our current data suggest involvement of Kir4.1 or GLT-1 with Rosenthal fibers or their abnormal localization.Rather, an overall decrease in protein expression is apparent. When proteasomal degradation is inhibited, abnormal GFAP

interactions lead to adaptive autophagy and increased lysosomal degradation (Tang et al., 2008) which may contribute to reduced protein levels of both membrane-bound proteins.

A threshold theory of GFAP toxicity has been speculated about in the literature for many years. In support of this, our data demonstrate that R236H transgenic animals which have no increase in GFAP in the spinal cord express normal expression levels of Kir4.1 and GLT-1. In contrast, $hGFAP^{TG}$ mice which show significant elevations in GFAP demonstrate marked decreases in Kir4.1 and GLT-1 protein. This is exacerbated when R236H animals are crossed with $hGFAP^{TG}$ mice, although the level of GFAP in this model is not elevated above that of $hGFAP^{TG}$ alone. This may be a specific example of the contribution of mutation to disease development. While a threshold of GFAP expression is necessary for Rosenthal fiber formation, this level is reduced in the presence of a mutation (Tanaka et al., 2007). It may be that Rosenthal fiber formation, rather than total GFAP, is key to pathology.

Although protein aggregates are the hallmark pathology of AxD, their relative toxicity and contribution to pathology has been debated. In the case of GFAP upregulation, accumulation, and aggregation, Rosenthal fibers may be both a result of aberrant GFAP filament formation as well as a contributor to further pathology. As described in the introduction, increased GFAP expression leading to Rosenthal fiber formation induces stress-related JNK activation and interaction with the 20S subunit contributes to proteasome inhibition. Toxicity of Rosenthal fibers is supported by data that suggests *in vitro* primary astrocytes that express mutant GFAP only produce significant cell death in cells that have large, perinuclear aggregates (Mignot et al., 2007). AlphaB-crystallin (Cryab), a small heat shock protein that regulates GFAP assembly, is

consistently elevated in AxD (Iwaki et al., 1989; Iwaki et al., 1993). In mouse models of AxD, loss of Cryab results in increased mortality, whereas elevation protects animals from terminal seizures (Hagemann et al., 2009). Transgenic over-expression of Cryab in $hGFAP^{TG}/R236H^{-/+}$ mice results in reduced CNS stress response, restored expression of GLT-1, and protects these animals from premature death (Hagemann et al., 2009). Additionally, Cryab effectively reduces the size of mutant GFAP oligomers to smaller oligomers and monomers, which reverses proteasomal inhibition and encourages GFAP degradation (Tang et al., 2010). These data suggest that large, oligomeric forms of GFAP are particularly toxic.

Decreasing oligomer size with Cryab does not eliminate the possibility of a toxic intermediate in the GFAP polymerization process, which has been suggested (Li et al., 2002) similar to other protein aggregate disorders. Supporting this, changes in migration in mutant GFAP transfected U251 cells far outweighed the presence of Rosenthal fibers, which only formed in about 3% of cells (Yoshida et al., 2007). Additionally, Cho and Messing (2008) found that cultured $hGFAP^{TG}$ astrocytes show changes in cell division, hydrogen peroxide sensitivity, and viability that were disproportionate to the number of cells forming aggregates. It is possible that both an intermediate and aggregated form of GFAP have contributions to pathology. The pathways for normal filament formation and aberrant aggregation are not mutually exclusive, and rates are continually dependent upon available GFAP monomer levels as well as a number of interacting proteins (Tian et al., 2006; Mignot et al., 2007; Li et al., 2002).

As mentioned, the identification of mutations in GFAP as the causative agent in AxD was a serendipitous one. In efforts to better understand processes of astrogliosis

associated with elevated GFAP, overexpressing mouse lines were generated (Messing et al., 1998). The highest expressing lines displayed widespread Rosenthal fiber formation and early mortality-the pathological hallmark of AxD. Since this initial discovery, the lower GFAP expressing line, $hGFAP^{TG}$ has been utilized as a primary model for AxD. Our data indicate, at least in caudal brain regions, a loss of K^+ and glutamate homeostasis downstream of GFAP overexpression may contribute to disease pathology. These animals, however, display mild phenotypes and the changes we see may represent sub-clinical or pre-symptomatic alterations that may be found with other causes of gliosis.

Gene regulation and gliosis

We and others have demonstrated developmental expression of astrocytic proteins GFAP, Kir4.1, and GLT-1 share a similar temporal induction in early postnatal development which tightly parallels increasing transcript levels for each gene. Further, we show a strong inverse correlation between decreased mRNA and protein expression for both Kir4.1 and GLT-1 with elevated GFAP expression. Our data indicate that prior to loss of Kir4.1 and GLT-1 protein, their mRNAs are decreased. We see this in two graded models of AxD mice. This is not unique to AxD and is also seen where GFAP is elevated but no aggregates are observed. Together, these data suggest, at least in part, transcriptional mechanisms are involved. At this point, the mechanisms by which GFAP forms specific interactions leading to transcriptional changes remain unexplored.

It is possible that one contributing mechanism to transcriptional changes in AxD is conserved across multiple neurodegenerative diseases. For example, a number of neurological disorders featuring protein aggregates have implicated TAR DNA-binding

protein 43 (TDP-43), as a key regulator in disease pathogenesis, including ALS and frontotemporal dementia (FTLD-TDP) (Neumann et al., 2006). TDP-43 is an RNA and DNA binding protein with many functions ultimately affecting both transcription and translation (for review see Lee et al. (2012). Originally identified for its binding to chromosomally integrated trans-activation response element (TAR) DNA and transcriptional repression of HIV-1, TDP-43 has also been shown to be involved with pre-mRNA splicing and translational regulation. In association with protein aggregates, TDP-43 has been shown to mislocalize from the nucleus to the cytoplasm and form insoluble inclusions in ALS (Neumann et al., 2006) and other neurodegenerative conditions including Alzheimer's, Parkinson's, and Huntington's diseases (Nakashima-Yasuda et al., 2007;Schwab et al., 2008;Uryu et al., 2008). Interestingly, cytoplasmic aggregate localization of TDP-43 has also been identified in Rosenthal fibers in pilocytic astrocytoma (Lee et al., 2008) and, very recently, AxD (Walker et al., 2014). Mislocalization of TDP-43 to the cytoplasm functionally inhibits its normal roles in regulating gene expression. As increasing literature suggests pathological significance of TDP-43 dysfunction associated with protein aggregation, it is likely also involved in AxD pathology. Specifically, TDP-43 accumulation in response to oxidative stress is dependent on JNK activation (Meyerowitz et al., 2011), which may implicate TDP-43 in the feed-forward cycle previously discussed (Tang et al., 2006;Wang et al., 2010). As increased GFAP induces oxidative stress and activates JNK, cytosolic TDP-43 accumulation is then facilitated. Removal of TDP-43 from the nucleus would presumably induce changes seen with lack of TDP-43, which results in increased GFAP (Polymenidou et al., 2011), providing an additional feed-forward pathway. Additionally,

involvement of TDP-43 in the pathology of AxD may provide a mechanism by which increased GFAP leads to persistent downregulation of Kir4.1 and GLT-1 gene transcripts. Specifically, TDP-43 binds the GLT-1 gene *SLC1A2* directly (Polymenidou et al., 2011) and Rosenthal fiber mislocalization of TDP-43 would persistently alter downstream gene expression indefinitely as these aggregates have not been shown to resolve once developed, as suggested by the threshold theory for AxD, which suggests that once met, GFAP protein accumulation or aggregation initiates an irreversible course of pathology. On the spectrum of reactivity of astrocytes, there may exist a similar threshold that determines whether or not gliosis is reversible (Sofroniew, 2009), placing GFAP in a role as a 'master regulator' in gliosis and providing a therapeutic gene target that would benefit a wide variety of CNS insults.

Heterogeneity and autonomy

The heterogeneity of protein expression observed between astrocytes located in spinal cord and cortex may be a reflection of the tissue in which they are located and the specific functional requirements of astrocytes (Emsley and Macklis, 2006). For example, Kir4.1 is expressed at high levels in the ventral gray matter of rat spinal cord surrounding large, high frequency-firing motor neurons., Lower levels are expressed in the dorsal horn, which contains unmyelinated and slower discharging sensory pathways (Olsen et al., 2007). Such astrocytic variability between functional regions may be associated with plasticity of astrocytes to the surrounding environment (Oberheim et al., 2012). Physiologically, basal and evoked K^+ concentrations are higher in dorsal gray matter, while astrocytic resting membrane potential is depolarized and K^+ uptake currents are

reduced relative to ventral, reflecting the differences in Kir4.1 expression (Olsen et al., 2007). The facility of astrocytic plasticity is possibly best demonstrated by reactivity to injury and the dependence of the response to injury conditions (Sofroniew, 2009;Oberheim et al., 2012). Though there is clear potential for astrocytic plasticity, its contribution to tissue-specific heterogenieity is difficult to determine. Evidence for multiple astrocyte progenitors and contributions of cell lineage to heterogeneous astrocyte populations continues to grow.

Cell lineage tracing studies have revealed a number of distinct progenitor cell types that give rise to astrocytes across the CNS. We now know that forebrain astrocytes not only originate from radial glial cells found in the ventricular zone, but also from subventricular zone glial progenitor cells, and $NG2^{+}$ progenitor cells (Oberheim et al., 2012). This diversity of cellular origin is thought to be reflected in part in the heterogeneity ultimately observed in mature astrocytes. Spinal cord astrocytes are generated from a distinct, and similarly varied set of progenitors. Olig2 progenitors of the ventral ventricular zone give rise to ventral astrocytes, oligodendrocytes and motor neurons, while three distinct domains of the ventral ventricular zone regionally produce astrocyte subpopulations throughout the cord (Oberheim et al., 2012). Heterogeneity of lineage and phenotype indicate a morphogenic origin of distinct astrocyte populations, and indicate epigenetic mechanisms regulate persistent differences in astrocyte populations.

Important to this idea is the maintenance of varying expression profiles in comparative cultures. Indeed, we see similar differences in protein expression maintained in cultures from $hGFAP^{TG}$ spinal cord (Fig.10) and cortical astrocytes (data not shown),

further suggesting astrocytic origin has a strong impact on gene expression, independent of external factors. These cell autonomous differences between spinal cord and cortical astrocytes isolated from hGFAP^{TG} mice also suggest that different populations of astrocytes may respond differently to the same gliosis-inducing stimuli. It is possible that the differences in astrocytes from the cortex and spinal cord underlie the two distinct types of Alexander disease in response to the same mutation. Our data suggest Kir4.1 is differentially regulated in the cortex and spinal cord in response to increased GFAP. Both increased and decreased Kir4.1 channel function have been implicated in disease. It is possible that this channel contributes to both types of AxD by two distinct mechanisms.

Utilizing *in vitro* methods, we have begun further exploring the regulatory role of GFAP on astrocytes. Plasmid-induced overexpression of GFAP in primary cultured astrocytes provides another important tool to assess the temporal effects of GFAP on astrocytes. Acute induction of GFAP, as opposed to developmental expression in cultured hGFAP^{TG} astrocytes, removes confounds associated with possible interruptions of developmental pathways. Conversely, using shRNA constructs targeting GFAP, we see a dose-dependent reduction of GFAP in primary cultured astrocytes (data not shown). This technique is currently being implemented to target both mouse and human GFAP independently and in tandem in hGFAP^{TG} cultured spinal cord astrocytes to assess the necessity of GFAP for the maintenance of the cellular phenotype. Our data suggest that GFAP is sufficient to induce long-term expression changes in astrocytes, but does it continue to regulate these pathways? We are currently using these tools to explore the notion that reduction of GFAP reverses phenotypes associated with AxD and gliosis, including the loss of Kir4.1 and GLT-1, and to provide evidence for a causal relationship.

We believe these studies will provide valuable insight to symptoms observed in those with type II AxD, as well provide information regarding gliosis in the broader context of CNS diseases.

GENERAL REFERENCE LIST

Anderson CM, Swanson RA (2000) Astrocyte glutamate transport: review of properties, regulation, and physiological functions. Glia 32:1-14.

Balbi P, Seri M, Ceccherini I, Uggetti C, Casale R, Fundaro C, Caroli F, Santoro L (2008) Adult-onset Alexander disease : report on a family. J Neurol 255:24-30.

Bandyopadhyay U, Sridhar S, Kaushik S, Kiffin R, Cuervo AM (2010) Identification of regulators of chaperone-mediated autophagy. Mol Cell 39:535-547.

Barres BA (2008) The mystery and magic of glia: a perspective on their roles in health and disease. Neuron 60:430-440.

Benkler C, Ben-Zur T, Barhum Y, Offen D (2013) Altered astrocytic response to activation in SOD1(G93A) mice and its implications on amyotrophic lateral sclerosis pathogenesis. Glia 61:312-326.

Bergles DE, Jahr CE (1997) Synaptic activation of glutamate transporters in hippocampal astrocytes. Neuron 19:1297-1308.

Bockenhauer D, et al. (2009) Epilepsy, ataxia, sensorineural deafness, tubulopathy, and KCNJ10 mutations. N Engl J Med 360:1960-1970.

Bordey A, Sontheimer H (1998) Properties of human glial cells associated with epileptic seizure foci. Epilepsy Res 32:286-303.

Borrelli MJ, Carlini WG, Ransom BR, Dewey WC (1986) Ion-sensitive microelectrode measurements of free intracellular chloride and potassium concentrations in hyperthermia-treated neuroblastoma cells. J Cell Physiol 129:175-184.

Brenner M, Goldman JE, Quinlan RA, Messing A (2009) Alexander disease: a genetic disorder of astrocytes. In: Astrocytes in (patho)physiology of the nervous system (Parpura V, Haydon P, eds), pp 591-648. New York, NY: Springer.

Brenner M, Johnson AB, Boespflug-Tanguy O, Rodriguez D, Goldman JE, Messing A (2001) Mutations in GFAP, encoding glial fibrillary acidic protein, are associated with Alexander disease. Nat Genet 27:117-120.

Burda JE, Sofroniew MV (2014) Reactive gliosis and the multicellular response to CNS damage and disease. Neuron 81:229-248.

Cavelier P, Attwell D (2005) Tonic release of glutamate by a DIDS-sensitive mechanism in rat hippocampal slices. J Physiol 564:397-410.

Chin SS, Goldman JE (1996) Glial inclusions in CNS degenerative diseases. J Neuropathol Exp Neurol 55:499-508.

D'Ambrosio R, Maris DO, Grady MS, Winn HR, Janigro D (1999) Impaired K(+) homeostasis and altered electrophysiological properties of post-traumatic hippocampal glia. J Neurosci 19:8152-8162.

Der PM, Su M, Wen SF, Li R, Gibbon T, Prescott AR, Brenner M, Quinlan RA (2006) The Alexander disease-causing glial fibrillary acidic protein mutant, R416W, accumulates into Rosenthal fibers by a pathway that involves filament aggregation and the association of alpha B-crystallin and HSP27. Am J Hum Genet 79:197-213.

Diamond JS, Jahr CE (2000) Synaptically Released Glutamate Does Not Overwhelm Transporters on Hippocampal Astrocytes During High-Frequency Stimulation. Journal of Neurophysiology 83:2835-2843.

Djukic B, Casper KB, Philpot BD, Chin LS, McCarthy KD (2007) Conditional knock-out of Kir4.1 leads to glial membrane depolarization, inhibition of potassium and glutamate uptake, and enhanced short-term synaptic potentiation. J Neurosci 27:11354-11365.

Dunlop J, Beal MH, She Y, Howland DS (2003) Impaired spinal cord glutamate transport capacity and reduced sensitivity to riluzole in a transgenic superoxide dismutase mutant rat model of amyotrophic lateral sclerosis. J Neurosci 23:1688-1696.

Elobeid A, Bongcam-Rudloff E, Westermark B, Nister M (2000) Effects of inducible glial fibrillary acidic protein on glioma cell motility and proliferation. J Neurosci Res 60:245-256.

Emirandetti A, Graciele ZR, Sabha M, Jr., de Oliveira AL (2006) Astrocyte reactivity influences the number of presynaptic terminals apposed to spinal motoneurons after axotomy. Brain Res 1095:35-42.

Emsley JG, Macklis JD (2006) Astroglial heterogeneity closely reflects the neuronal-defined anatomy of the adult murine CNS. Neuron Glia Biol 2:175-186.

Eng LF, Lee YL, Kwan H, Brenner M, Messing A (1998) Astrocytes cultured from transgenic mice carrying the added human glial fibrillary acidic protein gene contain Rosenthal fibers. J Neurosci Res 53:353-360.

Etcheberrigaray E, Gibson GE, Alkon DL (1994) Molecular mechanisms of memory and the pathophysiology of Alzheimer's disease. Ann N Y Acad Sci 747:245-255.

Ferraro TN, Golden GT, Smith GG, Martin JF, Lohoff FW, Gieringer TA, Zamboni D, Schwebel CL, Press DM, Kratzer SO, Zhao H, Berrettini WH, Buono RJ (2004) Fine mapping of a seizure susceptibility locus on mouse Chromosome 1: nomination of Kcnj10 as a causative gene. Mamm Genome 15:239-251.

Filali M, Lalonde R, Rivest S (2011) Sensorimotor and cognitive functions in a SOD1(G37R) transgenic mouse model of amyotrophic lateral sclerosis. Behav Brain Res 225:215-221.

Flint D, Brenner M (2011) Alexander disease. In: Leukodystrophies (Raymond GV, Eichler F, Fatemi A, Naidu S, eds), pp 106-129. London: MacKeith Press.

Fort PE, Sene A, Pannicke T, Roux MJ, Forster V, Mornet D, Nudel U, Yaffe D, Reichenbach A, Sahel JA, Rendon A (2008) Kir4.1 and AQP4 associate with Dp71- and utrophin-DAPs complexes in specific and defined microdomains of Muller retinal glial cell membrane. Glia 56:597-610.

Goodrich GS, Kabakov AY, Hameed MQ, Dhamne SC, Rosenberg PA, Rotenberg A (2013) Ceftriaxone treatment after traumatic brain injury restores expression of the glutamate transporter, GLT-1, reduces regional gliosis, and reduces post-traumatic seizures in the rat. J Neurotrauma 30:1434-1441.

Gorospe JR, Maletkovic J (2006) Alexander disease and megalencephalic leukoencephalopathy with subcortical cysts: leukodystrophies arising from astrocyte dysfunction. Ment Retard Dev Disabil Res Rev 12:113-122.

Gorospe JR, Naidu S, Johnson AB, Puri V, Raymond GV, Jenkins SD, Pedersen RC, Lewis D, Knowles P, Fernandez R, De VD, van der Knaap MS, Messing A, Brenner M, Hoffman EP (2002) Molecular findings in symptomatic and pre-symptomatic Alexander disease patients. Neurology 58:1494-1500.

Graff-Radford J, Schwartz K, Gavrilova RH, Lachance DH, Kumar N (2014) Neuroimaging and clinical features in type II (late-onset) Alexander disease. Neurology 82:49-56.

Grass D, Pawlowski PG, Hirrlinger J, Papadopoulos N, Richter DW, Kirchhoff F, Hulsmann S (2004) Diversity of functional astroglial properties in the respiratory network. J Neurosci 24:1358-1365.

Hagemann TL, Boelens WC, Wawrousek EF, Messing A (2009) Suppression of GFAP toxicity by alphaB-crystallin in mouse models of Alexander disease. Hum Mol Genet 18:1190-1199.

Hagemann TL, Connor JX, Messing A (2006) Alexander disease-associated glial fibrillary acidic protein mutations in mice induce Rosenthal fiber formation and a white matter stress response. J Neurosci 26:11162-11173.

Hazell AS, Rao KV, Danbolt NC, Pow DV, Butterworth RF (2001) Selective down-regulation of the astrocyte glutamate transporters GLT-1 and GLAST within the medial thalamus in experimental Wernicke's encephalopathy. J Neurochem 78:560-568.

Hedlund E (2011) The protective effects of beta-lactam antibiotics in motor neuron disorders. Exp Neurol 231:14-18.

Hinterkeuser S, Schroder W, Hager G, Seifert G, Blumcke I, Elger CE, Schramm J, Steinhauser C (2000) Astrocytes in the hippocampus of patients with temporal lobe epilepsy display changes in potassium conductances. Eur J Neurosci 12:2087-2096.

Howard KL, Hall DA, Moon M, Agarwal P, Newman E, Brenner M (2008) Adult-onset Alexander disease with progressive ataxia and palatal tremor. Mov Disord 23:118-122.

Huang K, Kang MH, Askew C, Kang R, Sanders SS, Wan J, Davis NG, Hayden MR (2010) Palmitoylation and function of glial glutamate transporter-1 is reduced in the YAC128 mouse model of Huntington disease. Neurobiol Dis 40:207-215.

Hughes EG, Maguire JL, McMinn MT, Scholz RE, Sutherland ML (2004) Loss of glial fibrillary acidic protein results in decreased glutamate transport and inhibition of PKA-induced EAAT2 cell surface trafficking. Brain Res Mol Brain Res 124:114-123.

Ingram EM, Wiseman JW, Tessler S, Emson PC (2001) Reduction of glial glutamate transporters in the parietal cortex and hippocampus of the EL mouse. J Neurochem 79:564-575.

Iwaki T, Iwaki A, Tateishi J, Sakaki Y, Goldman JE (1993) Alpha B-crystallin and 27-kd heat shock protein are regulated by stress conditions in the central nervous system and accumulate in Rosenthal fibers. Am J Pathol 143:487-495.

Iwaki T, Kume-Iwaki A, Liem RK, Goldman JE (1989) Alpha B-crystallin is expressed in non-lenticular tissues and accumulates in Alexander's disease brain. Cell 57:71-78.

Jany PL, Hagemann TL, Messing A (2013) GFAP expression as an indicator of disease severity in mouse models of Alexander disease. ASN Neuro 5:e00109.

Johnson AB (1996) Alexander disease . In: Handbook of clinical neurology , Moser, H.W. (ed.) pp 701 – 710. Amsterdam : Elsevier Science B.V .

Kaiser M, Maletzki I, Hulsmann S, Holtmann B, Schulz-Schaeffer W, Kirchhoff F, Bahr M, Neusch C (2006) Progressive loss of a glial potassium channel (KCNJ10) in the spinal cord of the SOD1 (G93A) transgenic mouse model of amyotrophic lateral sclerosis. J Neurochem 99:900-912.

Khakh BS, Sofroniew MV (2014) Astrocytes and Huntington's Disease. ACS Chem Neurosci.

Kimelberg HK, Nedergaard M (2010) Functions of astrocytes and their potential as therapeutic targets. Neurotherapeutics 7:338-353.

Kiryk A, Aida T, Tanaka K, Banerjee P, Wilczynski GM, Meyza K, Knapska E, Filipkowski RK, Kaczmarek L, Danysz W (2008) Behavioral characterization of GLT1 (+/-) mice as a model of mild glutamatergic hyperfunction. Neurotox Res 13:19-30.

Kofuji P, Ceelen P, Zahs KR, Surbeck LW, Lester HA, Newman EA (2000) Genetic Inactivation of an Inwardly Rectifying Potassium Channel (Kir4.1 Subunit) in Mice: Phenotypic Impact in Retina. J Neurosci 20:5733-5740.

Koller H, Schroeter M, Jander S, Stoll G, Siebler M (2000) Time course of inwardly rectifying K(+) current reduction in glial cells surrounding ischemic brain lesions. Brain Res 872:194-198.

Kucheryavykh YV, Kucheryavykh LY, Nichols CG, Maldonado HM, Baksi K, Reichenbach A, Skatchkov SN, Eaton MJ (2007) Downregulation of Kir4.1 inward rectifying potassium channel subunits by RNAi impairs potassium transfer and glutamate uptake by cultured cortical astrocytes. Glia 55:274-281.

Lee EB, Lee VM, Trojanowski JQ (2012) Gains or losses: molecular mechanisms of TDP43-mediated neurodegeneration. Nat Rev Neurosci 13:38-50.

Lee EB, Lee VM, Trojanowski JQ, Neumann M (2008) TDP-43 immunoreactivity in anoxic, ischemic and neoplastic lesions of the central nervous system. Acta Neuropathol 115:305-311.

Lehre KP, Danbolt NC (1998) The number of glutamate transporter subtype molecules at glutamatergic synapses: chemical and stereological quantification in young adult rat brain. J Neurosci 18:8751-8757.

Lein ES, et al. (2007) Genome-wide atlas of gene expression in the adult mouse brain. Nature 445:168-176.

Li Q, Zhang R, Guo YL, Mei YW (2009) Effect of neuregulin on apoptosis and expressions of STAT3 and GFAP in rats following cerebral ischemic reperfusion. J Mol Neurosci 37:67-73.

Li R, Johnson AB, Salomons G, Goldman JE, Naidu S, Quinlan R, Cree B, Ruyle SZ, Banwell B, D'Hooghe M, Siebert JR, Rolf CM, Cox H, Reddy A, Gutierrez-Solana LG, Collins A, Weller RO, Messing A, van der Knaap MS, Brenner M (2005) Glial fibrillary acidic protein mutations in infantile, juvenile, and adult forms of Alexander disease. Ann Neurol 57:310-326.

Li R, Messing A, Goldman JE, Brenner M (2002) GFAP mutations in Alexander disease. Int J Dev Neurosci 20:259-268.

Liedtke W, Edelmann W, Bieri PL, Chiu FC, Cowan NJ, Kucherlapati R, Raine CS (1996) GFAP is necessary for the integrity of CNS white matter architecture and long-term maintenance of myelination. Neuron 17:607-615.

Liedtke W, Edelmann W, Chiu FC, Kucherlapati R, Raine CS (1998) Experimental autoimmune encephalomyelitis in mice lacking glial fibrillary acidic protein is characterized by a more severe clinical course and an infiltrative central nervous system lesion. Am J Pathol 152:251-259.

Liss B, Haeckel O, Wildmann J, Miki T, Seino S, Roeper J (2005) K-ATP channels promote the differential degeneration of dopaminergic midbrain neurons. Nat Neurosci 8:1742-1751.

Liu D, Pitta M, Lee JH, Ray B, Lahiri DK, Furukawa K, Mughal M, Jiang H, Villarreal J, Cutler RG, Greig NH, Mattson MP (2010) The KATP channel activator diazoxide ameliorates amyloid-beta and tau pathologies and improves memory in the 3xTgAD mouse model of Alzheimer's disease. J Alzheimers Dis 22:443-457.

MacFarlane SN, Sontheimer H (1997) Electrophysiological changes that accompany reactive gliosis in vitro. J Neurosci 17:7316-7329.

Mangiarini L, Sathasivam K, Seller M, Cozens B, Harper A, Hetherington C, Lawton M, Trottier Y, Lehrach H, Davies SW, Bates GP (1996) Exon 1 of the HD gene with an expanded CAG repeat is sufficient to cause a progressive neurological phenotype in transgenic mice. Cell 87:493-506.

Maragakis NJ, Rothstein JD (2004) Glutamate transporters: animal models to neurologic disease. Neurobiol Dis 15:461-473.

Martin PM, O'Callaghan JP (1995) A direct comparison of GFAP immunocytochemistry and GFAP concentration in various regions of ethanol-fixed rat and mouse brain. J Neurosci Methods 58:181-192.

Martinez L, de LS (2007) Astrocytic reaction to a lesion, under hormonal deprivation. Neurosci Lett 415:190-193.

McAdoo DJ, Xu G, Robak G, Hughes MG, Price EM (2000) Evidence that reversed glutamate uptake contributes significantly to glutamate release following experimental injury to the rat spinal cord. Brain Res 865:283-285.

McCall MA, Gregg RG, Behringer RR, Brenner M, Delaney CL, Galbreath EJ, Zhang CL, Pearce RA, Chiu SY, Messing A (1996) Targeted deletion in astrocyte intermediate filament (Gfap) alters neuronal physiology. Proc Natl Acad Sci U S A 93:6361-6366.

Meisingset TW, Risa O, Brenner M, Messing A, Sonnewald U (2010) Alteration of glial-neuronal metabolic interactions in a mouse model of Alexander disease. Glia 58:1228-1234.

Messing A, Brenner M (2003) Alexander disease: GFAP mutations unify young and old. Lancet Neurol 2:75.

Melzer N, Meuth SG, Torres-Salazar D, Bittner S, Zozulya AL, Weidenfeller C, Kotsiari A, Stangel M, Fahlke C, Wiendl H (2008) A beta-lactam antibiotic dampens excitotoxic inflammatory CNS damage in a mouse model of multiple sclerosis. PLoS One 3:e3149.

Messing A, Head MW, Galles K, Galbreath EJ, Goldman JE, Brenner M (1998a) Fatal encephalopathy with astrocyte inclusions in GFAP transgenic mice. Am J Pathol 152:391-398.

Messing A, Head MW, Galles K, Galbreath EJ, Goldman JE, Brenner M (1998b) Fatal encephalopathy with astrocyte inclusions in GFAP transgenic mice. Am J Pathol 152:391-398.

Meyerowitz J, Parker SJ, Vella LJ, Ng DC, Price KA, Liddell JR, Caragounis A, Li QX, Masters CL, Nonaka T, Hasegawa M, Bogoyevitch MA, Kanninen KM, Crouch PJ, White AR (2011) C-Jun N-terminal kinase controls TDP-43 accumulation in stress granules induced by oxidative stress. Mol Neurodegener 6:57.

Middeldorp J, Hol EM (2011) GFAP in health and disease. Prog Neurobiol 93:421-443.

Mignot C, Delarasse C, Escaich S, Della GB, Noe E, Colucci-Guyon E, Babinet C, Pekny M, Vicart P, Boespflug-Tanguy O, Dautigny A, Rodriguez D, Pham-Dinh D (2007) Dynamics of mutated GFAP aggregates revealed by real-time imaging of an astrocyte model of Alexander disease. Exp Cell Res 313:2766-2779.

Nakashima-Yasuda H, et al. (2007) Co-morbidity of TDP-43 proteinopathy in Lewy body related diseases. Acta Neuropathol 114:221-229.

Nawashiro H, Brenner M, Fukui S, Shima K, Hallenbeck JM (2000) High susceptibility to cerebral ischemia in GFAP-null mice. J Cereb Blood Flow Metab 20:1040-1044.

Neumann M, Sampathu DM, Kwong LK, Truax AC, Micsenyi MC, Chou TT, Bruce J, Schuck T, Grossman M, Clark CM, McCluskey LF, Miller BL, Masliah E, Mackenzie IR, Feldman H, Feiden W, Kretzschmar HA, Trojanowski JQ, Lee VM (2006) Ubiquitinated TDP-43 in frontotemporal lobar degeneration and amyotrophic lateral sclerosis. Science 314:130-133.

Neusch C, Weishaupt JH, Bahr M (2003) Kir channels in the CNS: emerging new roles and implications for neurological diseases. Cell Tissue Res 311:131-138.

Neusch C, Rozengurt N, Jacobs RE, Lester HA, Kofuji P (2001) Kir4.1 Potassium Channel Subunit Is Crucial for Oligodendrocyte Development and In Vivo Myelination. J Neurosci 21:5429-5438.

Nwaobi SE, Lin E, Peramsetty SR, Olsen ML (2014) DNA methylation functions as a critical regulator of Kir4.1 expression during CNS development. Glia 62:411-427.

Oberheim NA, Goldman SA, Nedergaard M (2012) Heterogeneity of astrocytic form and function. Methods Mol Biol 814:23-45.

Olsen ML, Campbell SC, McFerrin MB, Floyd CL, Sontheimer H (2010a) Spinal cord injury causes a wide-spread, persistent loss of Kir4.1 and glutamate transporter 1: benefit of 17 beta-oestradiol treatment. Brain 133:1013-1025.

Olsen ML, Campbell SC, McFerrin MB, Floyd CL, Sontheimer H (2010b) Spinal cord injury causes a wide-spread, persistent loss of Kir4.1 and glutamate transporter 1: benefit of 17 beta-oestradiol treatment. Brain 133:1013-1025.

Olsen ML, Campbell SL, Sontheimer H (2007) Differential Distribution of Kir4.1 in Spinal Cord Astrocytes Suggests Regional Differences in K+ Homeostasis. Journal of Neurophysiology 98:786-793.

Olsen ML, Higashimori H, Campbell SL, Hablitz JJ, Sontheimer H (2006) Functional expression of Kir4.1 channels in spinal cord astrocytes. Glia 53:516-528.

Olsen ML, Sontheimer H (2008) Functional implications for Kir4.1 channels in glial biology: from K+ buffering to cell differentiation. J Neurochem 107:589-601.

Palfreyman JW, Thomas DG, Ratcliffe JG, Graham DI (1979) Glial fibrillary acidic protein (GFAP): purification from human fibrillary astrocytoma, development and validation of a radioimmunoassay for GFAP-like immunoactivity. J Neurol Sci 41:101-113.

Pappas TC, Alagarsamy S, Pollard RB, Nokta M (1998) HIV decreases glutamate transport in SK-N-MC neuroblastoma cells. J Neurovirol 4:69-79.

Pareyson D, Fancellu R, Mariotti C, Romano S, Salmaggi A, Carella F, Girotti F, Gattellaro G, Carriero MR, Farina L, Ceccherini I, Savoiardo M (2008) Adult-onset Alexander disease: a series of eleven unrelated cases with review of the literature. Brain 131:2321-2331.

Pekny M, Eliasson C, Chien CL, Kindblom LG, Liem R, Hamberger A, Betsholtz C (1998a) GFAP-deficient astrocytes are capable of stellation in vitro when cocultured with neurons and exhibit a reduced amount of intermediate filaments and an increased cell saturation density. Exp Cell Res 239:332-343.

Pekny M, Nilsson M (2005) Astrocyte activation and reactive gliosis. Glia 50:427-434.

Pekny M, Pekna M (2004) Astrocyte intermediate filaments in CNS pathologies and regeneration. J Pathol 204:428-437.

Pekny M, Stanness KA, Eliasson C, Betsholtz C, Janigro D (1998b) Impaired induction of blood-brain barrier properties in aortic endothelial cells by astrocytes from GFAP-deficient mice. Glia 22:390-400.

Pellerin L, Magistretti PJ (1994) Glutamate uptake into astrocytes stimulates aerobic glycolysis: a mechanism coupling neuronal activity to glucose utilization. Proc Natl Acad Sci U S A 91:10625-10629.

Perez-Alvarez MJ, Maza MC, Anton M, Ordonez L, Wandosell F (2012) Post-ischemic estradiol treatment reduced glial response and triggers distinct cortical and hippocampal signaling in a rat model of cerebral ischemia. J Neuroinflammation 9:157.

Pivonkova H, Benesova J, Butenko O, Chvatal A, Anderova M (2010) Impact of global cerebral ischemia on K+ channel expression and membrane properties of glial cells in the rat hippocampus. Neurochem Int 57:783-794.

Polymenidou M, Lagier-Tourenne C, Hutt KR, Huelga SC, Moran J, Liang TY, Ling SC, Sun E, Wancewicz E, Mazur C, Kordasiewicz H, Sedaghat Y, Donohue JP, Shiue L, Bennett CF, Yeo GW, Cleveland DW (2011) Long pre-mRNA depletion and RNA missplicing contribute to neuronal vulnerability from loss of TDP-43. Nat Neurosci 14:459-468.

Potokar M, Kreft M, Li L, Daniel AJ, Pangrsic T, Chowdhury HH, Pekny M, Zorec R (2007) Cytoskeleton and vesicle mobility in astrocytes. Traffic 8:12-20.

Potokar M, Stenovec M, Kreft M, Kreft ME, Zorec R (2008) Stimulation inhibits the mobility of recycling peptidergic vesicles in astrocytes. Glia 56:135-144.

Prust M, et al. (2011) GFAP mutations, age at onset, and clinical subtypes in Alexander disease. Neurology 77:1287-1294.

Raghavendra Rao VL, Rao AM, Dogan A, Bowen KK, Hatcher J, Rothstein JD, Dempsey RJ (2000) Glial glutamate transporter GLT-1 down-regulation precedes delayed neuronal death in gerbil hippocampus following transient global cerebral ischemia. Neurochem Int 36:531-537.

Ramos KM, Lewis MT, Morgan KN, Crysdale NY, Kroll JL, Taylor FR, Harrison JA, Sloane EM, Maier SF, Watkins LR (2010) Spinal upregulation of glutamate transporter GLT-1 by ceftriaxone: therapeutic efficacy in a range of experimental nervous system disorders. Neuroscience 169:1888-1900.

Ransom CB, Sontheimer H (1995) Biophysical and pharmacological characterization of inwardly rectifying K+ currents in rat spinal cord astrocytes. Journal of Neurophysiology 73:333-346.

Rao VL, Baskaya MK, Dogan A, Rothstein JD, Dempsey RJ (1998) Traumatic brain injury down-regulates glial glutamate transporter (GLT-1 and GLAST) proteins in rat brain. J Neurochem 70:2020-2027.

Reichold M, Zdebik AA, Lieberer E, Rapedius M, Schmidt K, Bandulik S, Sterner C, Tegtmeier I, Penton D, Baukrowitz T, Hulton SA, Witzgall R, Ben-Zeev B, Howie AJ, Kleta R, Bockenhauer D, Warth R (2010) KCNJ10 gene mutations causing EAST syndrome (epilepsy, ataxia, sensorineural deafness, and tubulopathy) disrupt channel function. Proc Natl Acad Sci U S A 107:14490-14495.

Rempe DA, Nedergaard M (2010) Targeting glia for treatment of neurological disease. Neurotherapeutics 7:335-337.

Rizzuto N, Ferrari G, Piscioli A (1980) Diffuse Rosenthal fiber formation in adults. A case report. Acta Neuropathol 50:237-240.

Rodriguez D, Gauthier F, Bertini E, Bugiani M, Brenner M, N'guyen S, Goizet C, Gelot A, Surtees R, Pedespan JM, Hernandorena X, Troncoso M, Uziel G, Messing A, Ponsot G, Pham-Dinh D, Dautigny A, Boespflug-Tanguy O (2001) Infantile Alexander disease: spectrum of GFAP mutations and genotype-phenotype correlation. Am J Hum Genet 69:1134-1140.

Romao LF, Sousa VO, Neto VM, Gomes FC (2008) Glutamate activates GFAP gene promoter from cultured astrocytes through TGF-beta1 pathways. J Neurochem 106:746-756.

Scholl UI, Choi M, Liu T, Ramaekers VT, Hausler MG, Grimmer J, Tobe SW, Farhi A, Nelson-Williams C, Lifton RP (2009) Seizures, sensorineural deafness, ataxia, mental retardation, and electrolyte imbalance (SeSAME syndrome) caused by mutations in KCNJ10. Proc Natl Acad Sci U S A 106:5842-5847.

Schwab C, Arai T, Hasegawa M, Yu S, McGeer PL (2008) Colocalization of transactivation-responsive DNA-binding protein 43 and huntingtin in inclusions of Huntington disease. J Neuropathol Exp Neurol 67:1159-1165.

Sechi G, Ceccherini I, Bachetti T, Deiana GA, Sechi E, Balbi P (2013) Ceftriaxone for Alexander's Disease: A Four-Year Follow-Up. JIMD Rep 9:67-71.

Sibson NR, Dhankhar A, Mason GF, Rothman DL, Behar KL, Shulman RG (1998) Stoichiometric coupling of brain glucose metabolism and glutamatergic neuronal activity. Proc Natl Acad Sci U S A 95:316-321.

Sicca F, Imbrici P, D'Adamo MC, Moro F, Bonatti F, Brovedani P, Grottesi A, Guerrini R, Masi G, Santorelli FM, Pessia M (2011) Autism with seizures and intellectual disability: possible causative role of gain-of-function of the inwardly-rectifying K+ channel Kir4.1. Neurobiol Dis 43:239-247.

Sofroniew MV (2009) Molecular dissection of reactive astrogliosis and glial scar formation. Trends Neurosci 32:638-647.

Sosunov AA, Guilfoyle E, Wu X, McKhann GM, Goldman JE (2013) Phenotypic conversions of "protoplasmic" to "reactive" astrocytes in Alexander disease. J Neurosci 33:7439-7450.

Srivastava R, Aslam M, Kalluri SR, Schirmer L, Buck D, Tackenberg B, Rothhammer V, Chan A, Gold R, Berthele A, Bennett JL, Korn T, Hemmer B (2012a) Potassium channel KIR4.1 as an immune target in multiple sclerosis. N Engl J Med 367:115-123.

Srivastava R, Aslam M, Kalluri SR, Schirmer L, Buck D, Tackenberg B, Rothhammer V, Chan A, Gold R, Berthele A, Bennett JL, Korn T, Hemmer B (2012b) Potassium channel KIR4.1 as an immune target in multiple sclerosis. N Engl J Med 367:115-123.

Steiner E, Enzmann GU, Lin S, Ghavampour S, Hannocks MJ, Zuber B, Ruegg MA, Sorokin L, Engelhardt B (2012) Loss of astrocyte polarization upon transient focal brain ischemia as a possible mechanism to counteract early edema formation. Glia 60:1646-1659.

Sullivan SM, Lee A, Bjorkman ST, Miller SM, Sullivan RK, Poronnik P, Colditz PB, Pow DV (2007a) Cytoskeletal anchoring of GLAST determines susceptibility to brain damage: an identified role for GFAP. J Biol Chem 282:29414-29423.

Sullivan SM, Macnab LT, Bjorkman ST, Colditz PB, Pow DV (2007b) GLAST1b, the exon-9 skipping form of the glutamate-aspartate transporter EAAT1 is a sensitive marker of neuronal dysfunction in the hypoxic brain. Neuroscience 149:434-445.

Sun HS, Feng ZP (2013) Neuroprotective role of ATP-sensitive potassium channels in cerebral ischemia. Acta Pharmacol Sin 34:24-32.

Tanaka H, Katoh A, Oguro K, Shimazaki K, Gomi H, Itohara S, Masuzawa T, Kawai N (2002) Disturbance of hippocampal long-term potentiation after transient ischemia in GFAP deficient mice. J Neurosci Res 67:11-20.

Tanaka K, Watase K, Manabe T, Yamada K, Watanabe M, Takahashi K, Iwama H, Nishikawa T, Ichihara N, Kikuchi T, Okuyama S, Kawashima N, Hori S, Takimoto M, Wada K (1997) Epilepsy and exacerbation of brain injury in mice lacking the glutamate transporter GLT-1. Science 276:1699-1702.

Tanaka KF, Takebayashi H, Yamazaki Y, Ono K, Naruse M, Iwasato T, Itohara S, Kato H, Ikenaka K (2007) Murine model of Alexander disease: analysis of GFAP aggregate formation and its pathological significance. Glia 55:617-631.

Tang G, Xu Z, Goldman JE (2006) Synergistic effects of the SAPK/JNK and the proteasome pathway on glial fibrillary acidic protein (GFAP) accumulation in Alexander disease. J Biol Chem 281:38634-38643.

Tian R, Wu X, Hagemann TL, Sosunov AA, Messing A, McKhann GM, Goldman JE (2010) Alexander disease mutant glial fibrillary acidic protein compromises glutamate transport in astrocytes. J Neuropathol Exp Neurol 69:335-345.

Tomita H, Shakkottai VG, Gutman GA, Sun G, Bunney WE, Cahalan MD, Chandy KG, Gargus JJ (2003) Novel truncated isoform of SK3 potassium channel is a potent dominant-negative regulator of SK currents: implications in schizophrenia. Mol Psychiatry 8:524-35, 460.

Tong XA, Ao Y, Nwaobi SE, Xu J, Haustein MA, Anderson MA, Mody I, Olsen ML, Sofronview MV, Khakh BS (2014) Huntington's disease model mice exhibit astrocyte Kir4.1 ion channel dysfunction that contributes to medium spiny neuron dysfunction.

Trotti D, Aoki M, Pasinelli P, Berger UV, Danbolt NC, Brown RH, Jr., Hediger MA (2001) Amyotrophic lateral sclerosis-linked glutamate transporter mutant has impaired glutamate clearance capacity. J Biol Chem 276:576-582.

Uryu K, Nakashima-Yasuda H, Forman MS, Kwong LK, Clark CM, Grossman M, Miller BL, Kretzschmar HA, Lee VM, Trojanowski JQ, Neumann M (2008) Concomitant TAR-DNA-binding protein 43 pathology is present in Alzheimer disease and corticobasal degeneration but not in other tauopathies. J Neuropathol Exp Neurol 67:555-564.

van der Knaap MS (2001) Magnetic resonance in childhood white-matter disorders. Dev Med Child Neurol 43:705-712.

Walker AK, Daniels CM, Goldman JE, Trojanowski JQ, Lee VM, Messing A (2014) Astrocytic TDP-43 pathology in Alexander disease. J Neurosci 34:6448-6458.

Wang X, Fan H, Ying Z, Li B, Wang H, Wang G (2010) Degradation of TDP-43 and its pathogenic form by autophagy and the ubiquitin-proteasome system. Neurosci Lett 469:112-116.

Wang Z, Pekarskaya O, Bencheikh M, Chao W, Gelbard HA, Ghorpade A, Rothstein JD, Volsky DJ (2003) Reduced expression of glutamate transporter EAAT2 and impaired glutamate transport in human primary astrocytes exposed to HIV-1 or gp120. Virology 312:60-73.

Weir MD, Thomas DG (1984) Effect of dexamethasone on glutamine synthetase and glial fibrillary acidic protein in normal and transformed astrocytes. Clin Neuropharmacol 7:303-306.

Wippold FJ, Perry A, Lennerz J (2006) Neuropathology for the neuroradiologist: Rosenthal fibers. AJNR Am J Neuroradiol 27:958-961.

Yamamoto A, Lucas JJ, Hen R (2000) Reversal of neuropathology and motor dysfunction in a conditional model of Huntington's disease. Cell 101:57-66.

Yang Y, Vidensky S, Jin L, Jie C, Lorenzini I, Frankl M, Rothstein JD (2011) Molecular comparison of GLT1+ and ALDH1L1+ astrocytes in vivo in astroglial reporter mice. Glia 59:200-207.

Ye ZC, Rothstein JD, Sontheimer H (1999) Compromised glutamate transport in human glioma cells: reduction-mislocalization of sodium-dependent glutamate transporters and enhanced activity of cystine-glutamate exchange. J Neurosci 19:10767-10777.

Yoshida T, Tomozawa Y, Arisato T, Okamoto Y, Hirano H, Nakagawa M (2007) The functional alteration of mutant GFAP depends on the location of the domain: morphological and functional studies using astrocytoma-derived cells. J Hum Genet 52:362-369.

Zamanian JL, Xu L, Foo LC, Nouri N, Zhou L, Giffard RG, Barres BA (2012) Genomic analysis of reactive astrogliosis. J Neurosci 32:6391-6410.

APPENDIX

INSTITUTIONAL ANIMAL CARE AND USE COMMITTEE APPROVAL FORM

THE UNIVERSITY OF ALABAMA AT BIRMINGHAM

Institutional Animal Care and Use Committee (IACUC)

NOTICE OF APPROVAL

DATE: June 6, 2014

TO: MICHELLE L OLSEN, D.Sc.
MCLM-958A
(205) 975-2715

FROM:

Robert A. Kesterson, Ph.D., Chair
Institutional Animal Care and Use Committee (IACUC)

SUBJECT: Title: Altered K+ Ion and Glutamate Homeostasis in Rett Syndrome
Sponsor: Rett Syndrome Research Foundation
Animal Project_Number: 140609409

As of June 6, 2014 the animal use proposed in the above referenced application is approved. The University of Alabama at Birmingham Institutional Animal Care and Use Committee (IACUC) approves the use of the following species and number of animals:

Species	Use Category	Number In Category
Mice	A	257
Mice	B	55
Rats	A	257
Rats	B	55

Animal use must be renewed by June 5, 2015. Approval from the IACUC must be obtained before implementing any changes or modifications in the approved animal use.

Please keep this record for your files, and forward the attached letter to the appropriate granting agency.

Refer to Animal Protocol Number (APN) 140609409 when ordering animals or in any correspondence with the IACUC or Animal Resources Program (ARP) offices regarding this study. If you have concerns or questions regarding this notice, please call the IACUC office at (205) 934-7692.

Institutional Animal Care and Use Committee (IACUC)
CH19 Suite 403
933 19th Street South
(205) 934-7692
FAX (205) 934-1188

Mailing Address:
CH19 Suite 403
1530 3rd Ave S
Birmingham, AL 35294-0019

THE UNIVERSITY OF ALABAMA AT BIRMINGHAM

Institutional Animal Care and Use Committee (IACUC)

MEMORANDUM

DATE: June 6, 2014

TO: MICHELLE L OLSEN, D.Sc.
MCLM-958A
(205) 975-2715

FROM:

Robert A. Kesterson, Ph.D., Chair
Institutional Animal Care and Use Committee (IACUC)

SUBJECT: **NOTICE OF APPROVAL - Please forward this notice to the appropriate granting agency.**

The following application was approved by the University of Alabama at Birmingham Institutional Animal Care and Use Committee (IACUC) on June 6, 2014.

Title: Altered K+ Ion and Glutamate Homeostasis in Rett Syndrome
Sponsor: Rett Syndrome Research Foundation

This institution has an Animal Welfare Assurance on file with the Office of Laboratory Animal Welfare (OLAW), is registered as a Research Facility with the USDA, and is accredited by the Association for Assessment and Accreditation of Laboratory Animal Care International (AAALAC).

Institutional Animal Care and Use Committee (IACUC)
CH19 Suite 403
933 19th Street South
(205) 934-7692
FAX (205) 934-1188

Mailing Address:
CH19 Suite 403
1530 3rd Ave S
Birmingham, AL 35294-0019